View metadata, citation and similar papers at core.ac.uk

brought to you by CORE

provided by Northumbria Research Link

Northumbria Research Link

Citation: Workman, David G., Hunter, Michael, Wang, Shuning, Brandel, Jérémy, Hubscher, Véronique, Dover, Lynn and Tetard, David (2020) The influence of linkages between 1-Hydroxy-2(1H)-pyridinone Coordinating Groups and a Tris(2-aminoethyl)amine core in a novel series of synthetic Hexadentate Iron(III) Chelators on antimicrobial activity. Bioorganic Chemistry, 95. p. 103465. ISSN 0045-2068

Published by: Elsevier

URL: https://doi.org/10.1016/j.bioorg.2019.103465 <https://doi.org/10.1016/j.bioorg.2019.103465>

This version was downloaded from Northumbria Research Link: http://nrl.northumbria.ac.uk/id/eprint/41658/

Northumbria University has developed Northumbria Research Link (NRL) to enable users to access the University's research output. Copyright © and moral rights for items on NRL are retained by the individual author(s) and/or other copyright owners. Single copies of full items can be reproduced, displayed or performed, and given to third parties in any format or medium for personal research or study, educational, or not-for-profit purposes without prior permission or charge, provided the authors, title and full bibliographic details are given, as well as a hyperlink and/or URL to the original metadata page. The content must not be changed in any way. Full items must not be sold commercially in any format or medium without formal permission of the copyright holder. The full policy is available online: http://nrl.northumbria.ac.uk/policies.html

This document may differ from the final, published version of the research and has been made available online in accordance with publisher policies. To read and/or cite from the published version of the research, please visit the publisher's website (a subscription may be required.)

Northumbria University
NEWCASTLE

University**Library**

The influence of linkages between 1-Hydroxy-2(1H)-pyridinone Coordinating Groups and a Tris(2-aminoethyl)amine core in a novel series of synthetic Hexadentate Iron(III) Chelators on antimicrobial activity.

David G. Workman[a], Michael Hunter[a], Shuning Wang[b,c], Jérémy Brandel[b,c], Véronique Hubscher[b,c], Lynn G. Dover[a], David Tétard[a]*

[a] Faculty of Health and Life Sciences, Northumbria University, Newcastle upon Tyne, NE1 8ST, United Kingdom.

[b] Université de Strasbourg, IPHC, 25 rue Becquerel 67087 Strasbourg, France

[c] CNRS, UMR7178, 67087 Strasbourg, France

Corresponding author: david.tetard@northumbria.ac.uk. Phone: Int + 44 (0)191 227 4934

Summary

Resistance of pathogens to antimicrobials is a major current healthcare concern. In a series of linked studies, we have investigated synthetic iron chelators based on hydroxy-pyridinone ligands as novel bacteriostatic agents. Herein we describe our synthesis of several useful building blocks based on the 1-hydroxy-2(1H)-pyridinone moiety, including a novel formyl derivative, which were combined with a tris(2-aminoethyl)amine core to obtain a series of new high-affinity hexadentate Fe(III) chelators. The design principle examined by this series is the size and flexibility of the linker between the core and the metal ligands. Measurement of the pKa and stability constants (Fe^{3+} and Cu^{2+}) of representative coordinating groups was performed to help rationalise the biological activity of the chelators. The novel chelators were tested on a panel of representative microorganisms with some effectively inhibiting microbial growth. We demonstrate that the nature and position of the linker between the hydroxypyridinone and the tris(2-aminoethyl)amine core has considerable impact upon microbial growth inhibition and that both amide or amine linkages can give efficacious chelators.

Keywords

Siderophore, Chelator, Biostatic agent, Bacterial Growth, 1-Hydroxy-2(1H)-pyridinone

1- Introduction

A major public health concern is the loss of activity of once efficacious antibiotics due to emerging bacterial resistance and its transfer among bacterial populations. The need to develop new antibiotics and new strategies to combat the spread of multi-drug resistant infections is pressing. It has long been known that metal chelators impose biostasis upon microorganisms. Their mode of action is thought to be the sequestration of the metal and subsequent starving of the microorganisms.[1-6]

For its biological importance, iron is an ideal primary target for metal withdrawal. In the case of infections, iron is plentiful in the body of the patient but is not readily available to the microorganism. The pathogen must compete with its host to mobilise iron.[7-9] Pathogenic microorganisms have evolved efficient iron acquisition mechanisms, the most remarkable one being based on small Fe^{3+} chelating molecules called siderophores, of which there are hundreds of examples.[10-11] The host employs various Fe^{3+} withholding strategies to limit bacterial growth including the production of the protein siderocalin that interferes with the siderophore-based iron acquisition.[12-14]

The majority of siderophores are hexadentate chelators; their Fe^{3+} affinities/binding strengths (as measured by pFe^{3+}[15] can be very high, in excess of 25.* They are thus able to acquire otherwise unavailable iron from sequestered host sources.[16-19] To complement the action of siderocalin in inhibiting siderophore -mediated iron uptake by pathogens, it is possible to envisage the therapeutic use of a synthetic chelator acting in the growth medium.

Alongside the difficulties associated with the design and synthesis of powerful therapeutic chelators is the risk of denaturation of essential metalloenzymes in the body of patients.[20-22] This and other factors complicate the development of anti-infective chelators. Further research and understanding of the effect of the structure of biostatic chelators on the thermodynamics and kinetics of binding of all relevant biological metals and their reactivity with human metalloenzymes are required.

* pFe^{3+} is defined as $-\log[Fe^{3+}]_{free}$, usually calculated at pH 7.4, with $[Chelator]_{total}$ = 10 μM and $[Fe^{3+}]_{total}$ = 1 μM and cited herein in these conditions.

The focus of our research is on the design of chelators for powerful Fe^{3+} chelation and competition with the high affinity iron uptake systems of pathogens, including siderophores, to complement the activities of antimicrobial compounds. To compete with bacterial siderophores (that are commonly based on coordinating groups such as α-hydroxycarboxylic acids, hydroxamic acids and catechols)[11, 18], it is crucial to select the right coordinating group. Focusing purely on thermodynamic aspects of metallation in competition between siderophores and another chelator, the respective pFe^{3+} of the two molecules is the key parameter to consider.[23] The pFe^{3+} value encompasses all the factors influencing the chelation of Fe^{3+}, including the structural parameters, pKa and stability constant(s). It would appear that three isomers of the bidentate hydroxypyridinone (HOPO) family (Figure 1) often endow hexadentate chelators with a good combination of pKa and $\log\beta(Fe^{3+})$ and therefore generate sufficiently high pFe^{3+} values.[19]

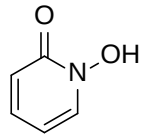

1-Hydroxy-2(1H)-pyridinone
(1,2-HOPO)

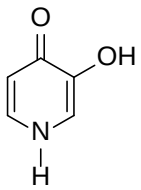

3-Hydroxy-4(1H)-pyridinone
(3,4-HOPO)

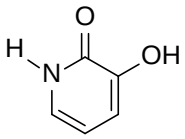

3-Hydroxy-2(1H)-pyridinone
(3,2-HOPO)

Figure 1. Three relevant isomers of the HOPO family.

Additional attractive properties can be expected through the use of HOPO coordinating groups. It is well known that many bacteria can exploit siderophores elaborated by other microbial species, a process called “siderophore piracy”.[9] In the proposed application, any synthetic chelator must not be recognised and taken up by pathogens to promote their growth.[6, 24] As very few HOPO are known in natural compounds and only one of the 1,2-HOPO class has been described as a siderophore, (the bidentate 1-hydroxy-5-methoxy-6-methyl-2(1H)-pyridinone also called cepabactin)[25] it is unlikely that metallated HOPO-based chelators will be recognised by bacterial receptors and exploited as a source of Fe^{3+}, but not impossible.[26] Furthermore, a therapeutic chelator must not interact with siderocalin either and thus inhibit its protective capacity. The binding between some 1,2-HOPO-based chelators and siderocalin has been studied and was found to be very weak, suggesting that this class of coordinating groups would not overwhelm this defence strategy, but rather may complement it.[27]

The most powerful Fe^{3+} chelator of the HOPO family is 3,4-HOPO.[28] Several hexadentate chelators based on that coordinating group, are also known to have antimicrobial action.[29-39] Interestingly, the opposite effect, i.e. promotion of the growth of *Escherichia coli* by an Fe^{3+} complex of a synthetic hexadentate 3,4-HOPO chelator has been observed[26] highlighting the need to fully understand the relationship in these chelators between structure and biological function.

We have recently described the first examples of biostatic hexadentate chelators based on 1,2-HOPO.[40] We considered that this class of HOPO may have advantages over the 3,4-HOPO isomers despite being predicted to be slightly weaker Fe^{3+} chelators.[28] For example, a lower pKa of the hydroxyl group in 1,2-HOPO may help limit host cell penetration and therefore may have advantages with respect to patient safety. To the best of our knowledge, until our first paper, only a very small number were known to contain at least one 1,2-HOPO moiety and these are illustrated in Figure 2.[27, 41-44]

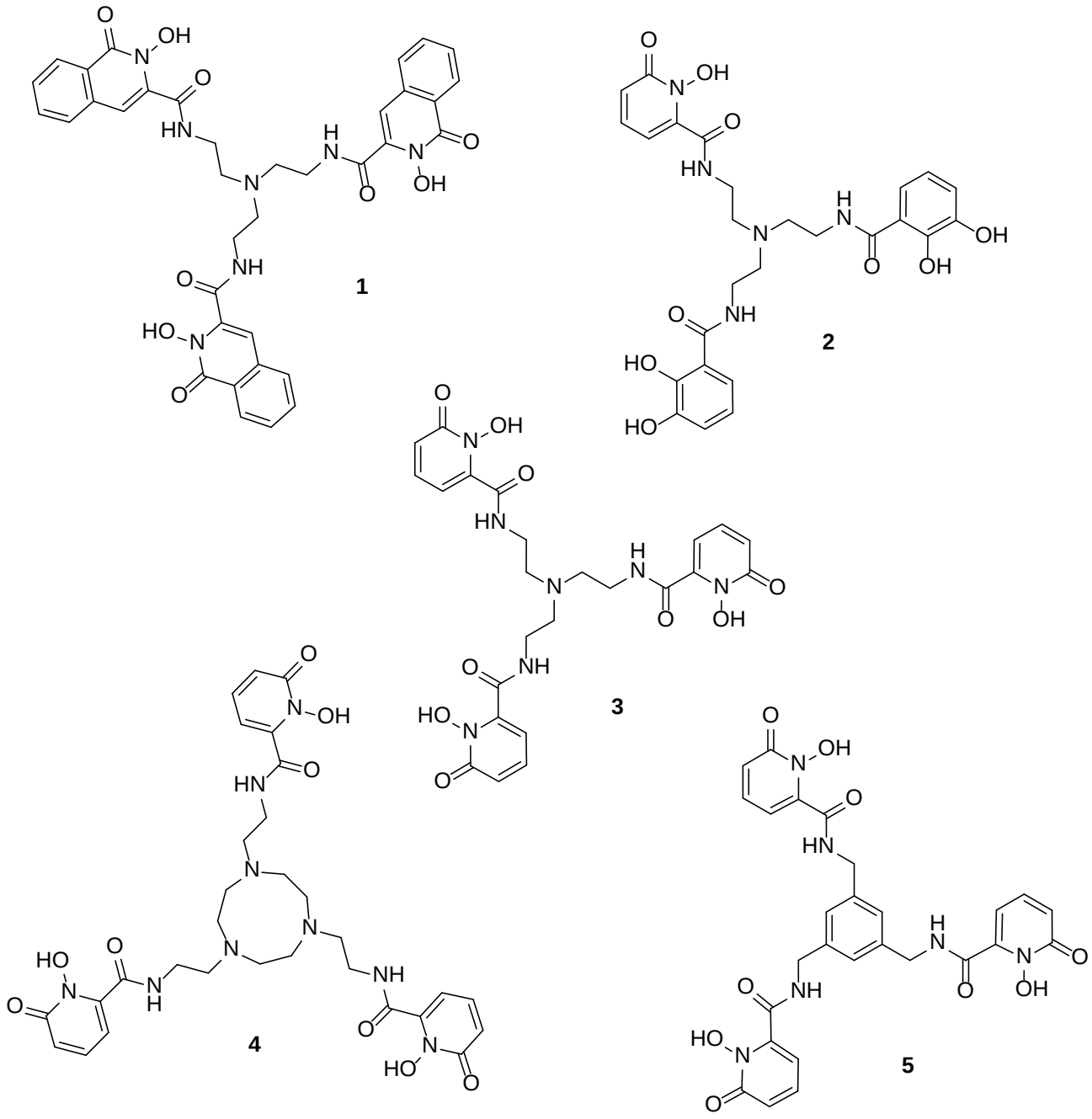

Figure 2. Hexadenate chelators based on 1,2-HOPO reported in the literature before Workman et al.[40]. **1** see ref [42]; **2** see ref [27]; **3** see ref [43]; **4** see ref [44]; **5** see ref [41].

Previously, our primary focus was to study the effect of the molecular backbone on biostatic activity rather than that of the linker between the 1,2-HOPO moiety and the backbone. Our promising results using a methylene linker between a 1,2-HOPO group and the 1,4,7-triazacyclonone backbone[40] prompted us to

investigate further the effect of linker structure in order to identify the most promising biostatic agents for further physicochemical and mechanistic studies. Of the previously known 1,2-HOPO-based hexadentate chelators on Figure 2, the focus is almost systematically on amide linkage on position 6 of the 1,2-HOPO ring. Studying other types of linkers may facilitate optimisation of the biostatic agent. A new hexadentate 1,2-HOPO-based chelator using a methylene linker was recently published by others.[45]

Here we report the synthesis of a range of hexadentate chelators bearing three 1,2-HOPO as coordinating groups anchored on a tris(2-aminoethyl)amine (TREN) core (Figure 3). This core has been used frequently in the synthesis of various hexadentate iron chelators based on HOPO and therefore selected here because it provides a common feature useful when comparing extant compounds.[29, 43, 45-47] Primarily, our novel chelators have been designed to explore novel systematic structural variations of the linkages between TREN and the hydroxypyridinone moiety, in particular secondary and tertiary amides, secondary and tertiary amines. Additionally, we show the effect of these chelators upon microbial growth. The contributory effect the linkages have on the chelation properties of the molecules i.e. pKa of the hydroxyl group, stability constants, will be reported separately.

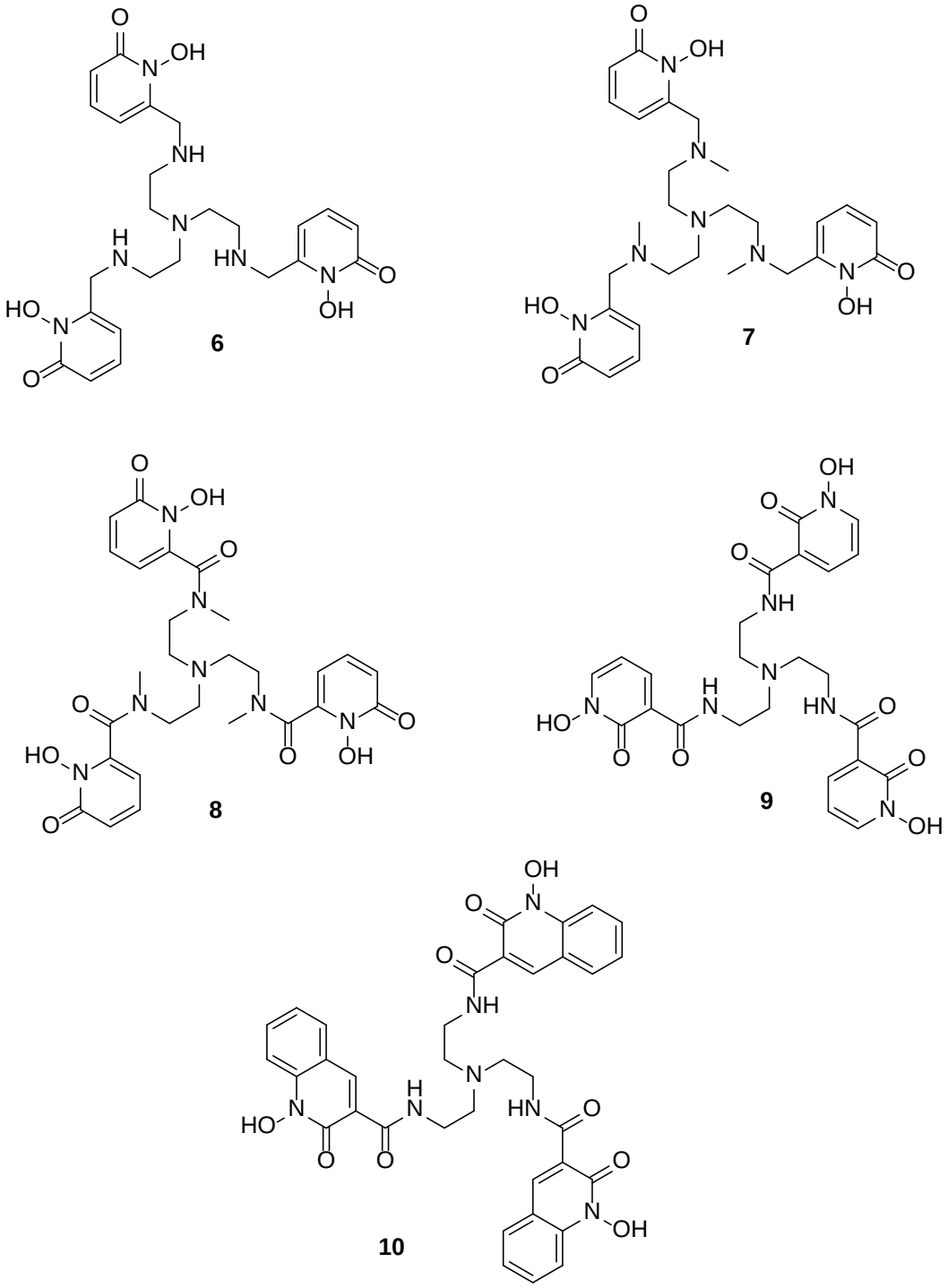

Figure 3. Novel chelators synthesised.

2- Results and Discussion

2.1 Synthesis

The access to our targeted chelators relied primarily on two key novel building blocks that were already available in our laboratory.[48] Firstly, starting from 2-hydroxy-pyridine-6-carboxylic acid 11 building block 12, i.e. 1-allyloxy-6-hydroxymethyl-2(1H)-pyridinone was easily obtained in four steps. Starting from 2-chloro-pyridine-3-carboxylic acid (13) the second key building block 14, i.e. 1-hydroxy-2(1H)-pyridinone-3-carboxylic acid was also easily obtained in two steps from (Scheme 1).

The choice of an allyl protective group of the 1-hydroxyl group of building block 11 and subsequent derivatives requires explanation. In order to expand the existing 1,2-HOPO chemistry to incorporate methylene-linked binding units into target multi-dentate chelate molecules (see below), a novel HOPO protection strategy instead of the traditionally used benzyloxy protection for 1,2-HOPO was required. Specifically, it was predicted that benzyl protection would not be suitable as the most common methods used for its removal would probably also cleave the linkage between our HOPO group and the molecular backbone. Of the protective methods identified, protection of the *N*-hydroxyl group as the allyloxy group was chosen. It was considered that deprotection could be achieved using a range of relatively mild conditions, for example *via* double bond isomerisation and subsequent hydrolysis without compromising other bonds in the chelator.[49]

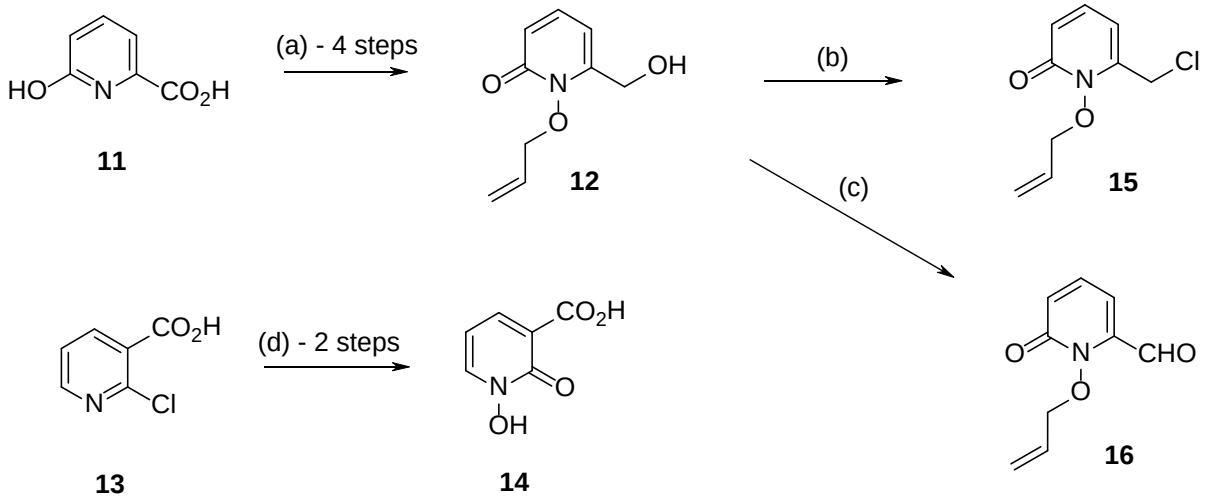

Scheme 1. (a) 4 steps: (i) CH_3CO_3H, acetic acid, heat (77%), (ii) $SOCl_2$, methanol, heat (96%), (iii) allyl bromide, K_2CO_3, acetonitrile, heat (94%), (iv) $NaBH_4$, methanol, THF, heat (65%) (b) $SOCl_2$, dichloromethane, heat (92%) (c) oxalyl chloride, DMSO, NEt_3, dichloromethane, 0^oC (33%) (d) 2 steps: (i) CH_3CO_3H, acetic acid, heat (42%) (ii) KOH, water, heat (92%).

The hydroxymethyl building block **12** could be converted to the novel chloromethyl derivative **15** and aldehyde **16** for incorporation onto the ligand cores. Novel isomer **14** of the original 1-hydroxy-2(1H)-pyridinone-6-carboxylic acid was required to assess any effect the regiochemistry has on the biological activity, with respect to the linker positioning that could have an impact on the pKa and metal stability constants (see below). With these novel building blocks in hand, it was then possible to build a more systematic series of hexadentate chelators based on 1,2-HOPOs.

Access to a more-flexible analogue of **3**, namely compound **6** (Scheme 2), where the carbonyl linking unit was replaced by a methylene group, was prepared following reductive amination of TREN (**17**) by aldehyde **16** in the presence of sodium borohydride, affording the triallyl-protected chelator **18** in poor yield (15%). Despite this yield, that method was preferable to direct alkylation of TREN using **15,** which resulted in an even lower yield (9%) attributed to excess alkylation of the amine pendant arms.

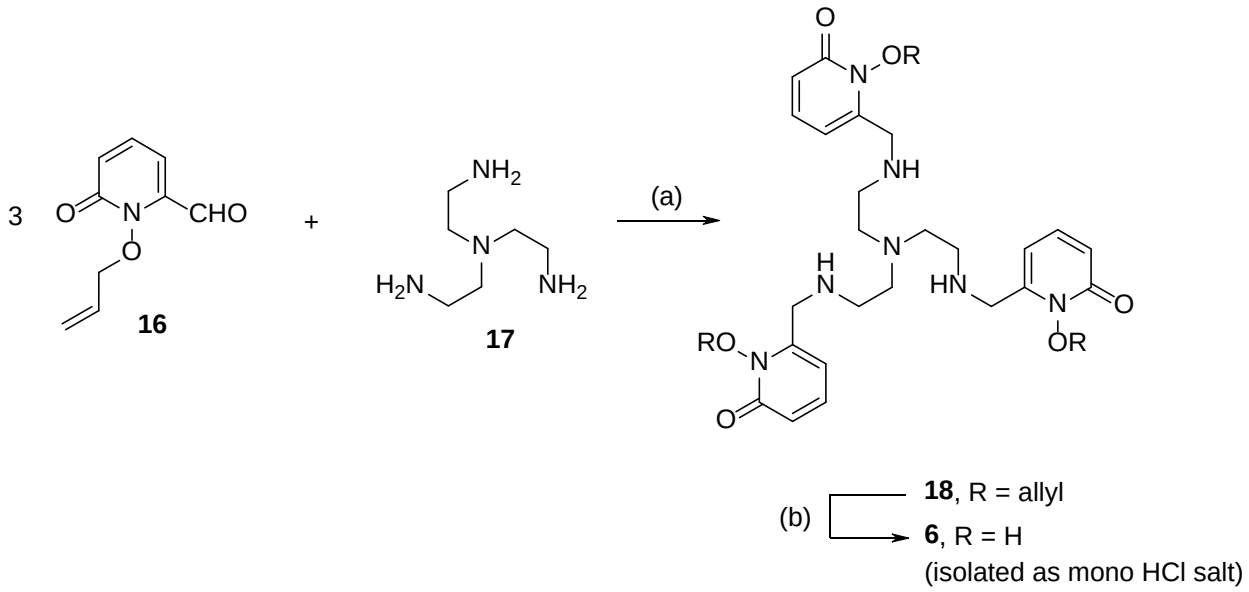

Scheme 2. Reagents and conditions: (a) (i) TREN, ethanol, heat, (ii) $NaBH_4$ (15%) (b) BCl_3, dichloromethane (75%).

Although removal of the allyl group using a HCl/AcOH mixture (a treatment that would be used to remove a benzyl protection) was possible, it also resulted in unacceptably frequent cleavage of the HOPO moiety from the TREN backbone. This problem was initially predicted and justified the need in our strategy for early identification of a different non-benzyl protective group. Attempts to deprotect **18** using Pd/C + TFA/1,4-dioxane [50] did not give chelator **6**. This was attributed to poisoning of the catalyst due to the presence of secondary amine groups. However, de-allylation of **18** using boron trichloride was successful and produced the novel secondary amine **6** in good yield (75%). As expected, an allyl protective group therefore proved very useful as at it was removed without cleavage of the methylene linker.

To further illustrate the versatility of the new building blocks, a tertiary amine linked chelator was designed. TREN was converted into tricarbamate **19** that was then reduced to a new backbone tris(N-methyl-2-aminoethyl)amine, or $(Me)_3$TREN **20**, by a previously reported procedure as shown in Scheme 3.[51]

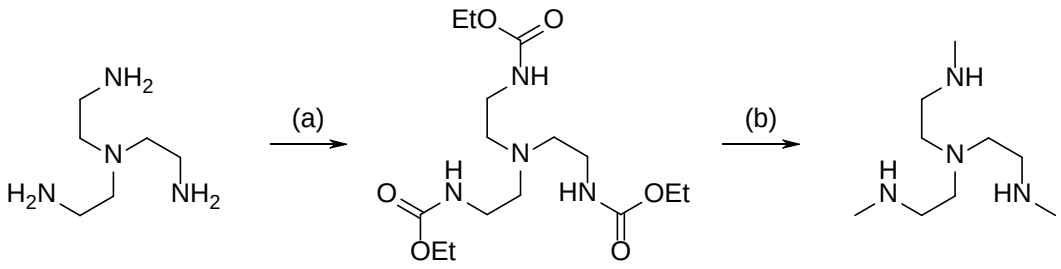

17 **19** **20**

Scheme 3. Reagents and conditions: (a) $ClCO_2Et$, KOH, toluene, 0°C (crude 92%) (b) (i) $LiAlH_4$, THF, heat (ii) KOH (19%).

Synthesis of **7** continued by the alkylation of **20** by chloromethyl 1,2-HOPO **15**, albeit in low yield (35%) (Scheme 4). Allyl removal from compound **21** using Pd/C catalyst in a 1,4-dioxane/TFA mixture afforded the novel chelator **7** in good yield (66%), without noticeable catalyst poisoning, again demonstrating the usefulness of using the allyl protective group in our synthetic strategy.

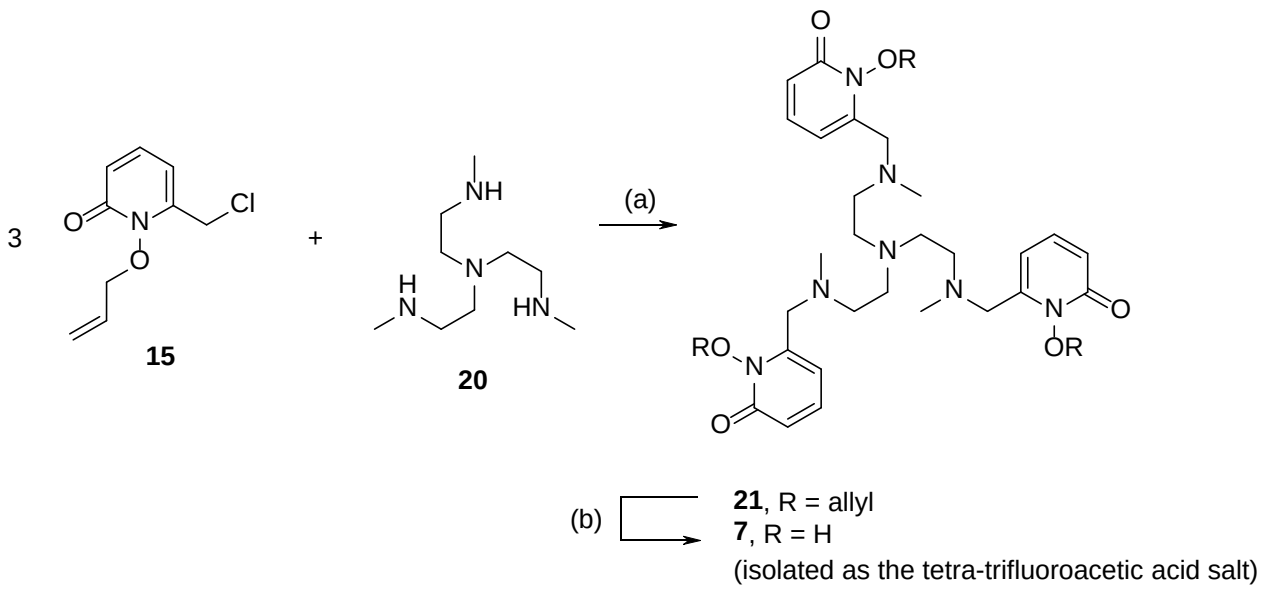

Scheme 4. Reagents and conditions: (a) K_2CO_3, acetonitrile, heat (35%) (b) Pd/C, TFA (0.17 M), 1,4-dioxane/water, heat (66%).

To complete the series of secondary and tertiary amines and amides necessary for biological testing, the synthesis of **3** was conducted as previously described[52] and the novel chelator **8** was synthesised as described in Scheme 5. Activation of known compound **22** as the acid chloride and subsequent coupling with **20** resulted in a poor yield. Instead, activation of **22** as the pentafluorophenol ester **23** was performed[53] and coupling with **20** gave **24** in a moderate yield (58%). Deprotection of **24** in a strong acid mixture afforded the desired novel chelator **8** in excellent yield (90%).

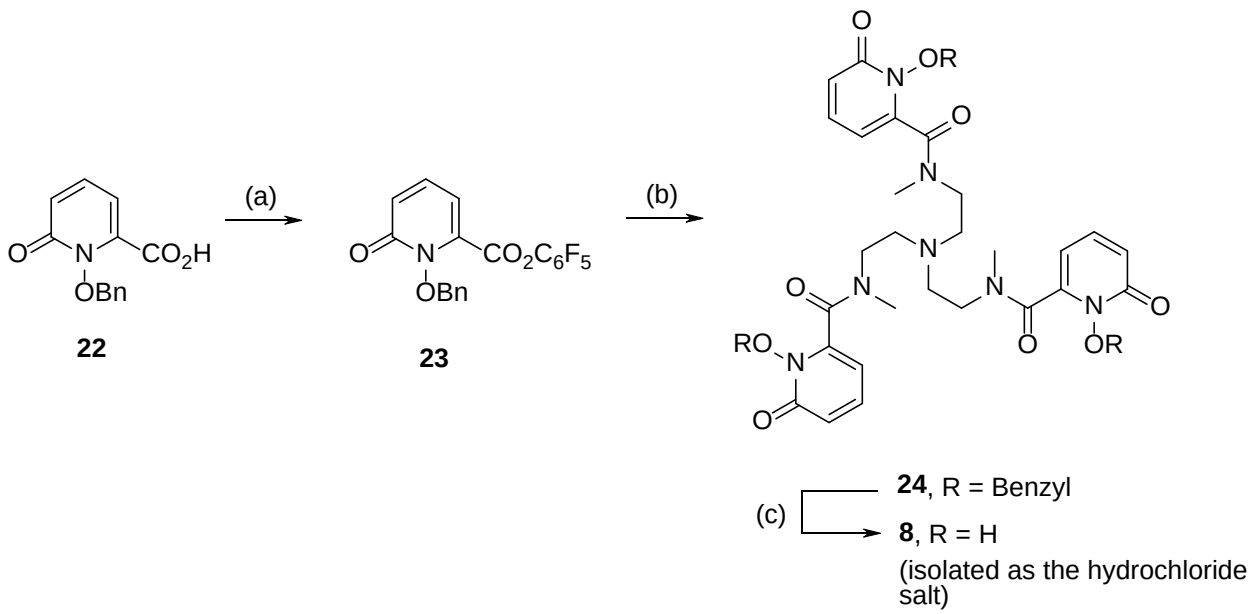

Scheme 5. Reagents and conditions: (a) $CF_3CO_2C_6F_5$, pyridine, DMF (b) **20**, $(^iPr)_2NEt$, DMF (58%) (c) HCl:AcOH (90%).

Following a slight modification of a method previously described by Raymond *et al.*[52], novel chelator **9**, the *retro* analogue of chelator **3** was synthesised (Scheme 6). Compound **14** was first benzyl-protected into **25** that was then converted to the mercaptothiazoline-activated derivative **26**. EDC (1-ethyl-3-(-3-dimethylaminopropyl)carbodiimide hydrochloride) was used instead of using DCC as the dehydrating agent in that latter step as we found removal of the reaction by-products was more easily accomplished. Coupling of **26** with TREN gave **27** that was deprotected in strongly acidic conditions (HCl:AcOH) to give chelator **9**. To the best of our knowledge, 9 is the first analogue of previously known hexadentate chelator **3** where the attachment point is in position 3 on the 1,2-HOPO ring.

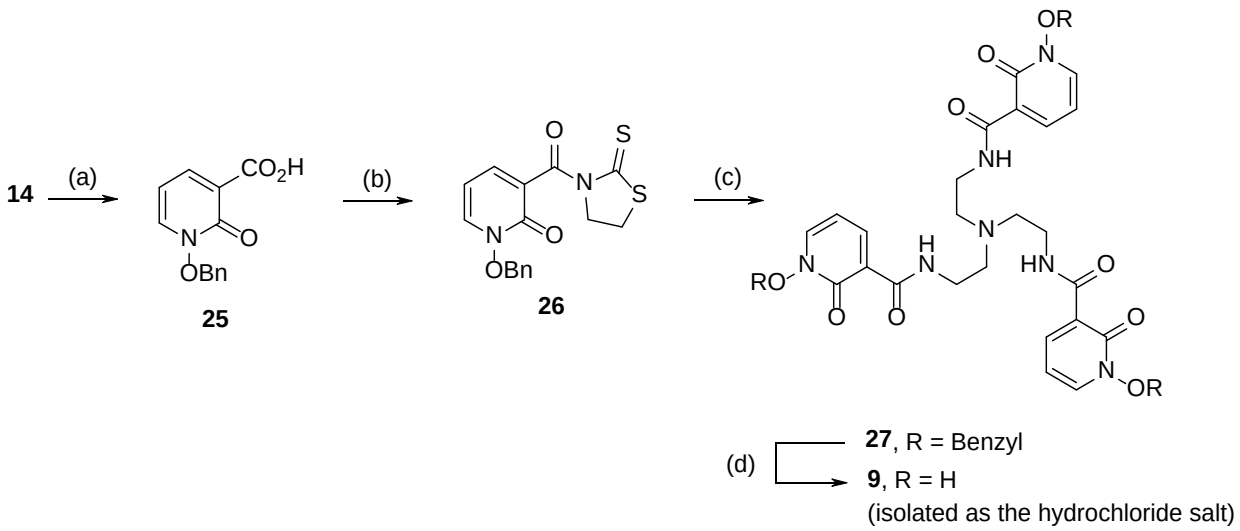

Scheme 6. Reagents and conditions: (a) benzyl bromide, K_2CO_3, methanol, heat (85%) (b) 2-Mercaptothiazoline, EDC, 4-(N,N-dimethylamino)pyridine (cat.), dichloromethane (44%) (c) TREN, dichloromethane (77%) (d) HCl:AcOH, 50°C (82%).

Because 1,2-HOPO moieties are isoelectronic to catechol (a frequently found coordinating group in bacterial siderophores), we considered that some of this series of chelators might be recognised by bacterial ferri-siderophore receptors akin to “siderophore piracy” (as previously shown for synthetic tris-catechol synthetic chelators). An undesirable effect of such recognition might be the promotion of bacterial growth.[54] We therefore sought analogues in which the 1,2-HOPO group would not resemble natural catechols. Two more analogues of compound **3** were synthesised containing fused benzene rings on the HOPO moiety. Besides its possible effect on the pKa and stability constant for Fe^{3+} (hence on pFe^{3+}), the extra aromatic ring might inhibit recognition of the ferric chelator by bacterial receptors. Compound **1** was synthesised as described previously.[55] A *retro* analogue of chelator **1**, namely compound **10** was also prepared from 1,2-HOPO derivative **28** (Scheme 7). Although compound **28** has long been known,[56] it was never been used in the synthesis of hexadentate metal chelators. Using the same method as for the synthesis of compound **1**, novel chelator **10** could be obtained in four steps from **28**.

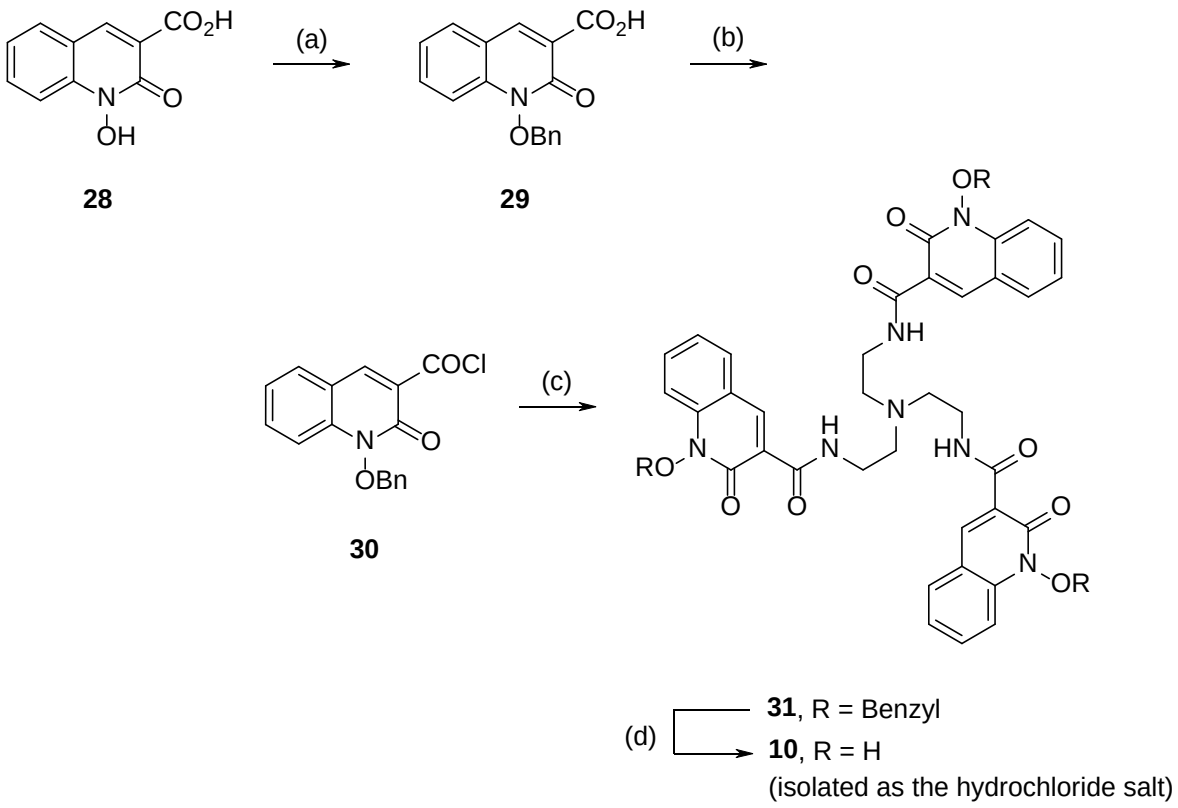

Scheme 7. Reagents and conditions: (a) Benzyl bromide, K_2CO_3, methanol, heat (83%) (b) Oxalyl chloride, DMF (cat.), toluene, 40°C (51%) (c) TREN, NEt_3, toluene (65%) (d) HCl:AcOH, 50°C (57%).

To test our hypothesis that chelator **3** and **9** limit the growth of bacteria via chelation in the growth medium rather than through other mechanisms linked to the TREN core after cell uptake, close analogues of these compounds where the coordinating groups were partially removed were considered desirable. Thus control compounds **32** and **33** were prepared as shown in Scheme 8.

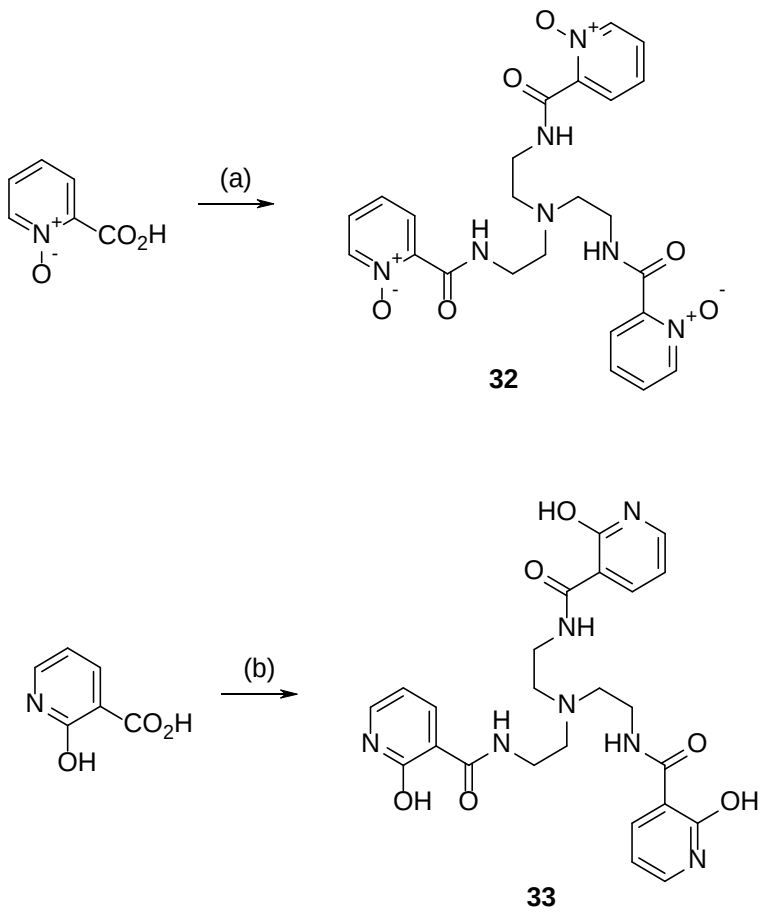

Scheme 8. Reagents and conditions: (a) HOBt, EDC, NEt_3, TREN, dichloromethane (32%) (b) TREN, PPh_3, $(C_5H_5NS)_2$, acetonitrile, 60°C (34%).

2.2 Physicochemical Properties

In order to assess the relative intrinsic metal binding affinity of the 1,2-HOPO coordinating group in compound **3** and **9** (positional isomers) without the thermodynamic influence of the backbone and without intramolecular hydrogen bonding and to assess their efficacy compared to 3,4-HOPO, their N,N-dimethyl amide analogues **34** and previously known **35**[57] were synthesised (Scheme 9). Their pKa and the stability constants of their Fe^{3+} and Cu^{2+} complexes were determined by potentiometric and spectrophotometric titrations.

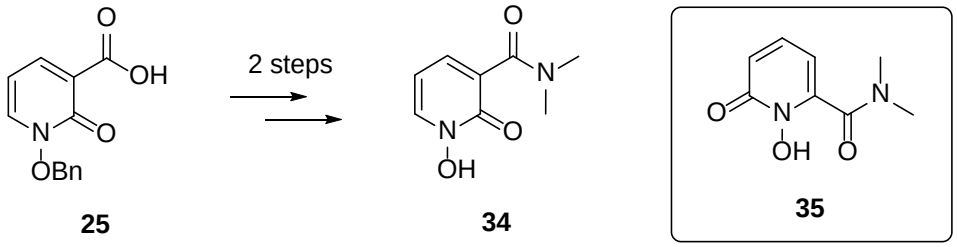

25 **34** **35**

Scheme 9. Synthesis of **34**. (i) oxalyl chloride, DMF (cat.), 60ºC then $(CH_3)_2NH$ (71%); (ii) H_2, Pd/C, HCl, Ethanol, Water (94%).

The spectrophotometric titration of ligands **35** versus pH (Figure 4) showed one band at 286 nm under very acidic pH (p[H]=-0.75, the brackets indicate that the values were not measured but calculated from p[H] = -log[H^+]). This band underwent a first bathochromic shift to 303 nm, then a second one to 324 nm. These variations suggest the presence of three species over the whole studied pH range, (**35**)H_2^+, (**35**)H and **35**.

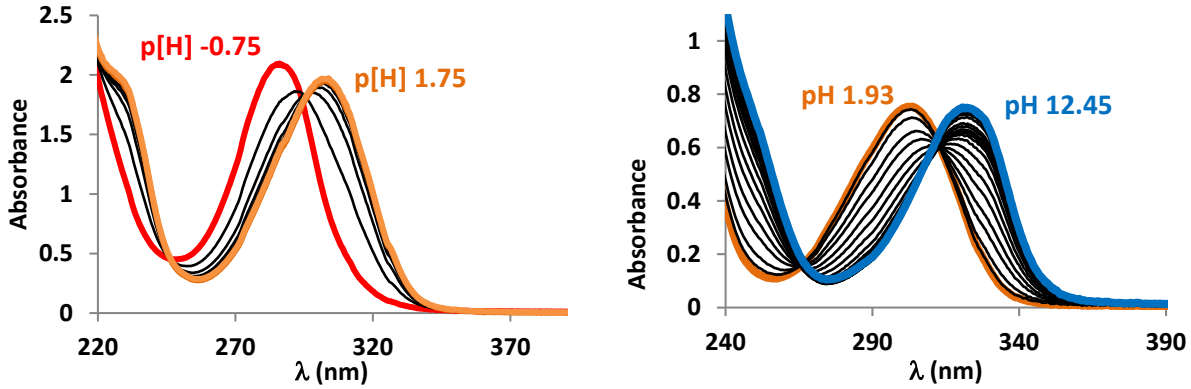

a) b)

Figure 4. Spectrophotometric titration versus pH of ligand **35** a) between p[H] -0.75 and 1.75 (batch), [**35**] = 3.08×10^{-4} M, and b) between pH 1.93 and 12.45, [**35**] = 1.18×10^{-4} M; *I* = 0.1 M ($NaClO_4$); T = 25.0(1)ºC; solvent: H_2O.

The fitting of the data allowed us to determine the acidity constants (p*K*a=- log *K*) of the two equilibria (Table 1) and to propose the protonation scheme (Scheme 10).

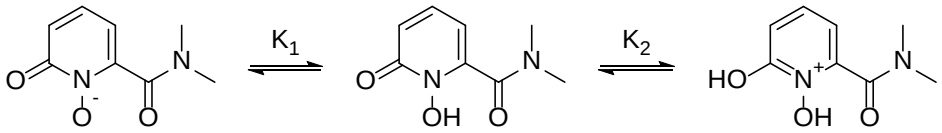

Scheme 10. Protonated species of ligand **35**.

Ligand **34** showed also one equilibrium in the 2-12 pH range (Figure S1b). Under very acidic pH, the hypochromic shift of the last two spectra suggested that the second protonation constant would be at much lower p[H] values (Figure S1a). The protonation constants allowed us to calculate the electronic spectra and the distribution curves of the protonated species of ligands **34** (Figure S2) and **35** (Figure 5), which showed that the ligands are in their totally deprotonated form $\mathbf{L}^-$ (**L**= **34**, **35**) at physiological pH (pH 7.4).

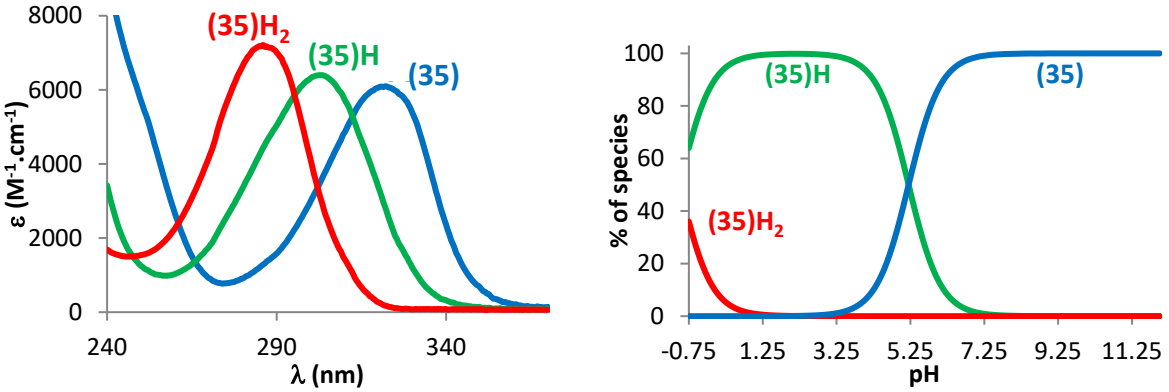

Figure 5. a) Electronic spectra and b) distribution curves ([**35**] = 2.5×10^{-4} M) of the protonated species of ligand **35**. *I* = 0.1 M ($NaClO_4$); T = 25.0(1)^{0}C; solvent: H_2O.

The hydroxyl group of chelator **35** is slightly more acidic than that of chelator **34**. This can probably be explained by the electronic effect of the substituent of the 6- and 3- position respectively and the existence of a bifurcated hydrogen bond in chelator **35**.

The complexation of Fe(III) by ligands **34** (Figure 5) and **35** (Figure S3) was then studied spectrophotometrically over the same pH range than the protonation studies. It showed for both ligands the appearance of a ligand-to-metal charge transfer band (LMCT) from very low pH that shifted hypsochromically when the pH increased up to around pH 6. Then, the LMCT band gradually decreased

and the baseline started increasing (see Figure 5b at 580 nm), sign that Fe(III) is released from the ligand and precipitating as $Fe(OH)_3$.

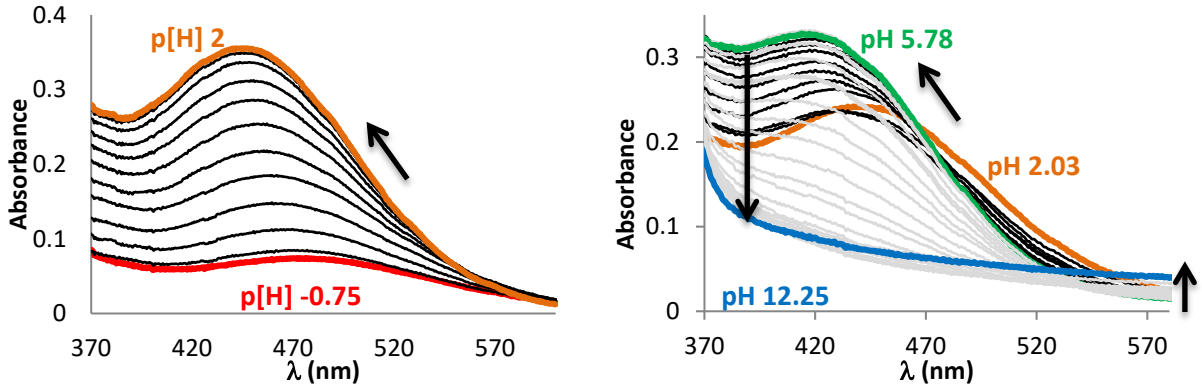

a) b)

Figure 6. Spectrophotometric titration versus pH of ligand **34** + Fe(III) ([**34**]/Fe(III) = 3.2) a) between p[H] -0.75 and 2.0 (batch), [**34**] = 3.01×10^{-4} M, and b) between pH 2.03 and 12.25, [**34**] = 2.34×10^{-4} M; *I* = 0.1 M ($NaClO_4$); T = 25.0(1)^{0}C; solvent: H_2O.

Data analysis allowed us to highlight the consecutive formation of FeL, FeL_2 and FeL_3 species for both ligands and their overall stability constants were calculated (Table 1). From these values, we calculated the electronic spectra and distribution curves of the complexes of ligands **34** (Figure 7b) and **35** (Figure S4) versus pH.

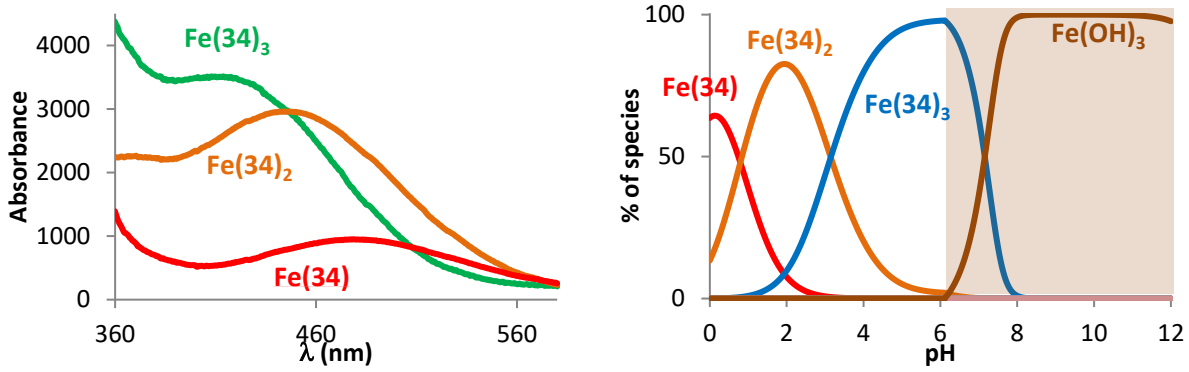

a) b)

Figure 7. a) electronic spectra and b) distribution curves of the Fe(III) complexes of ligand **34** ([**34**] = 2.5×10^{-4} M, $[\mathbf{34}]_{total}/[Fe]_{total}$ = 3.2); *I* = 0.1 M ($NaClO_4$); T = 25.0(1)^{0}C; solvent: H_2O.

The distribution curves of both ligands showed that, at physiological pH, Fe(III) would already be partially released from the bidentate ligands (25% Fe(**34**)$_3$, 75% Fe(OH)$_3$), what confirms the need to design hexadentate ligands by anchoring three bidentate units together.

Titrations of both ligands with Fe(III) were carried out at pH 2 (Figure S5) as well as competition experiments with EDTA in Hepes buffer at pH 7.4 (Figure S6). The conditional stability constants at fixed pH obtained from these experiments were converted to overall stability constants and were in good agreement with the one obtained from the titrations versus pH (Tables S1 and S2), confirming our complexation models. The complexation ability of both ligands with Cu(II) was studied by potentiometry and showed the formation of CuL and CuL$_2$ for both ligands.

Table 1. Protonation constants (p*K*a) of ligands **34** and **35**, overall stability constants (logβ_{mlh}) of their Fe(III) and Cu(II) complexes.

		Fe^{3+}			Cu^{2+}			
Ligand	p*K*a	logβ_{110}	logβ_{120}	logβ_{130}	logβ_{110}	logβ_{120}	logβ_{121}	logβ_{12-1}
34	5.40(3)	9.59(1)	18.06(1)	24.59(3)	6.2	11.0	/	/
35	5.20(3) (5.17[57]) ~0.4	9.99(2)	18.66(2)	25.88(3) (25.6[57])	6.3	11.6	/	/
1,2-HOPO[a]	5.78 -0.8	10.6	20.1	27.2	7.29(2)	13.06(3)	/	/
DFP[b]	9.82 3.64	15.01(1)	27.3(1)	37.43(1)	10.42(2)	19.09(1)	21.98(3)	8.49(3)

T = 25.0°C; solvent : water, *I* = 0.1 M ($NaClO_4$);
a. ref [58]
b. ref [59]

In order to compare the chelation power of the different ligands and their selectivity, the pM values were calculated from the overall stability constants and plotted against pH (Figure 8).

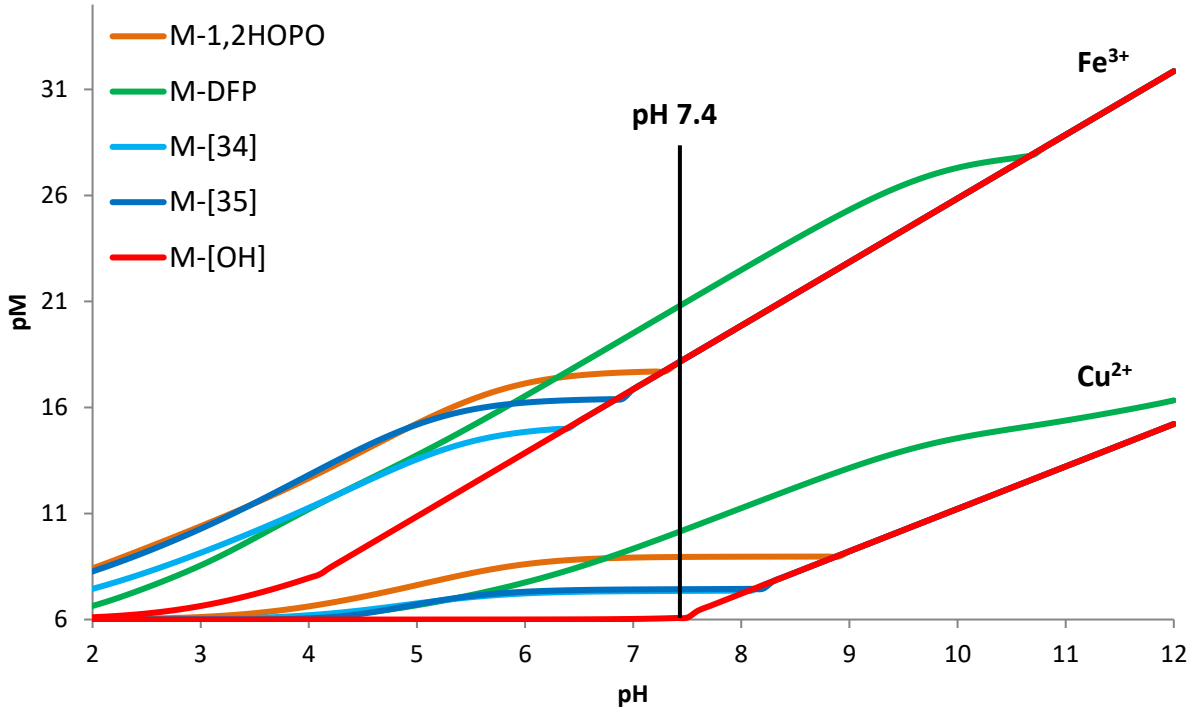

Figure 8. Chelation power (represented by the pM value) of the ligands versus pH. pM = -log$[M]_{free}$, $[L]_{total} = 10^{-5}$ M, $[M]_{total} = 10^{-6}$ M.

For a ligand to dominate metal chelation in aqueous media it must produce a pM curve (M= Fe(III), Cu(II)) above that of the hydroxide anion. The larger the difference, the stronger the chelator. between pH 2 and 5, ligand **35** and 1,2-HOPO are slightly better chelators than ligands **34** and DFP. From pH 6.3, DFP, based on the 3,4-HOPO chelating unit becomes a better chelator due to its higher p*K*a values. The calculated pCu^{2+} values showed that, as expected for 1,2-hydroxypyridinones bearing hard *O,O*-donors, the affinity for Fe^{3+} is much higher than for Cu^{2+}. These results suggested that these coordinating groups are suited for selective iron(III) chelation and that the synthesised hexadentate (tris-bidentate) chelators based on ligands **34** and **35** would achieve strong Fe(III) chelation and may primarily disrupt bacterial iron homeostasis.

2.3 Biological Activity

Broth microdilution tests were undertaken based upon a standard procedure.[60] in order to obtain minimum inhibitory concentrations (MICs, Table 2) for the synthetic ligands upon a range of Gram-negative and Gram-positive bacteria associated with HAIs, as well as the dimorphic fungus *Candida albicans*,. The commercially available DTPA (*N*,*N'*,*N'*,*N"*,*N"*-diethylenetriaminepentaacetic acid) and powerful synthetic Fe^{3+} chelator EMECAM (1,3,5-tris(2,3-dihydroxybenzamidomethyl)-2,4,6-triethylbenzene, pFe^{3+} = 32.6)[61-62] were also assayed for comparison. Finally, TACN-MeHP (1,4,7-tris(3-hydroxy-6-methyl-2-pyridylmethyl)-1,4,7-triazacyclononane, Figure 9), the most powerful Fe^{3+} chelator known (pFe^{3+} = 39.4) was used as an additional benchmark.[63]

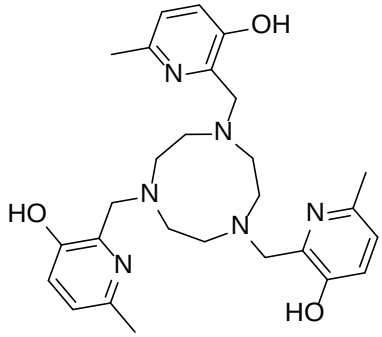

TACN-MeHP

Figure 9. 1,4,7-tris(3-hydroxy-6-methyl-2-pyridylmethyl)-1,4,7-triazacyclononane (TACN-MeHP).

Table 2. Minimum Inhibitory Concentrations (MIC) expressed in μM (in mg/L between brackets) for the ligands tested upon a panel of microorganisms. Results were determined in triplicate. The molar mass (g/mol) of each chelator is given between brackets in the first column.

Chelator (molar mass/g mol^{-1})	**Minimum Inhibitory Concentration / μM (mg/L)**						
	Gram-negative bacteria				Gram-positive bacteria		Fungus
	E. coli DSM-18039	*K. pneumoniae* DSM-30104	*P. aeruginosa* DSM-19880	*A. baumannii* DSM-30007	*B. subtilis* DSM-23778	*S. aureus* DSM-1104	*C. albicans* DSM-1386
DTPA (393.35)	2542 (1000)	2542 (1000)	>2542 (> 1000)	2542 (1000)	159 (62.5)	79 (31.1)	318 (125.1)
1 (744.16[b])	1250 (930.2)	1250 (930.2)	313 (232.9)	78 (58.0)	625 (465.1)	313 (232.9)	313 (232.9)
3 (593.98[b])	625 (348.5)	313 (174.5)	313 (174.5)	313 (174.5)	313 (174.5)	5 (2.8)	313 (174.5)
6 (552.03[b])	625 (345.0)	625 (345.0)	313 (172.8)	313 (172.8)	313 (172.8)	313 (172.8)	156 (86.1)
7 (1013.76[c])	1250 (1267)	2500 (2534)	625 (633.6)	313 (317.3)	625 (633.6)	625 (633.6)	78 (79.1)
8 (636.06[b])	5000 (3180)	>5000 (> 3180)	5000 (3180)	1250 (795.1)	625 (397.5)	625 (397.5)	156 (99.2)
9 (593.98[b])	2500 (1485)	5000 (2969.9)	2500 (1485)	313 (185.9)	313 (185.9)	5 (3.0)	313 (185.9)
10 (744.16[b])	1250 (930.2)	1250 (930.2)	625 (465.1)	313 (232.9)	625 (465.1)	156 (116.1)	625 (465.1)
32 (509.52)	>5000 (>2547)	>5000 (>2547)	>5000 (>2547)	>5000 (>2547)	>5000 (>2547)	>5000 (>2547)	>5000 (>2547)
33[a] (575.47)	>5000 (> 2877)	>5000 (> 2877)	>5000 (> 2877)	>5000 (> 2877)	>5000 (> 2877)	>5000 (> 2877)	>5000 (> 2877)
EMECAM (657.72)	3855 (2536)	1928 (1268)	1928 (1268)	1928 (1268)	1928 (1268)	482 (317.0)	>5000 (>3289)
TACN-MeHP (492.63)	78 (38.4)	313 (154.2)	625 (307.9)	156 (76.9)	78 (38.4)	78 (38.4)	39 (19.2)

(a) Due to solubility issues, the chelator was prepared by addition of three molar equivalents of aqueous sodium hydroxide before solvent removal and it was evaluated as the tri-sodium salt. (b) as HCl salt. (c) as tetra-trifluoroacetic acid salt.

Although the concept used in the design was for a series of synthetic chelators that mediated biostasis by a competitive extracellular iron limitation, it is possible that this series of compounds may enter the microbial cell and exert their effects by other mechanisms. The control compounds **32** and **33** were designed to highlight any biological activity of the TREN backbone and/or of the aromatic rings in compound **3** and **9** unconnected to their metal chelation activity if the compounds were nevertheless capable of penetrating the microorganisms. When tested, these control compounds caused no inhibition of bacterial growth at the concentrations used across the panel of microorganisms. This lack of activity therefore strongly suggests that compounds **3**, **9** and, by reasonable extension, the other chelators tested herein primarily exercise their growth inhibition activity through metal chelation and presumably in the growth medium.

When comparing the susceptibility of the tested microorganisms to each chelator (Table S3), some trends are evident. Such is the diversity of the cellular architecture, siderophore production capacity, siderophore identity and activity as well as transport system configurations represented in our panel of microorganisms, these differences in activity are likely multifactorial and require dedicated mechanistic study to resolve. In general, *C. albicans*, *S. aureus* and *B. subtilis* are the most sensitive microorganisms across the range of chelators used. The microorganisms that are least sensitive to these chelators are *K. pneumoniae* and *E. coli*. This trend is largely but not entirely systematic. For example, *C. albicans* is the most susceptible tested microorganism to compounds **6**, **7**, **8** and TACN-MeHP but it is also the least susceptible microorganism to EMECAM. We have observed the same trends in susceptibility (tested on the same microorganisms) on a related series of chelators based on 1,2-HOPO containing triaza macrocyclic cores, suggesting that a dominating factor for efficacy of our molecules is the coordinating group.[40] Also similar to our previous observation is the fact that of the microorganism tested, the Gram-positive bacteria and the fungus are more susceptible to the tested chelator than the Gram-negative bacteria. These latter Gram-negative bacteria possess an outer membrane that would provide some protection against water-soluble agents should they have an intracellular mode of action. This is not entirely assured as these membranes possess water-filled diffusion channels (porins) that could facilitate

our compounds' diffusion through this extra barrier. Additionally, all of these microorganisms also possess various drug efflux systems of various specificities. Interestingly, the strain of *B. subtilis* used is notably limited to the production of a bidentate siderophore[64],while both *E. coli* and *K. pneumoniae* are known to produce the very powerful siderophore enterobactin.[65-68] The kinetics of iron chelation expected in these different systems here are consistent with a model based upon extracellular iron chelation.

Hexadentate chelators based on 3,4-HOPO have been studied on their own (i.e. in the absence of added antimicrobial agents) as in the present study to inhibit bacterial growth.[29-31, 35] Contrary to our results, the authors did not find any significant difference between the susceptibility of Gram-positive and Gram-negative bacteria to their chelators. Whether the discrepancy between our results and theirs is due to the strains of microorganisms studied or due to the nature of the chelators remains to be established. The trend observed across the range of 1,2-HOPO-based chelators described herein and in our previous study[40] and the results of **32** and **33** are all wholly consistent with the hypothesis that metal chelation is key to biostatic effect. The few outliers in the trends of our MIC values (e.g. high efficacy of DTPA against *S. aureus*, compound **9** being one of the most efficacious against *S. aureus* but one of the poorest against *K. pneumoniae*) also suggest that thermodynamically driven Fe^{3+} chelation is not the only effect that influences growth of the microorganism. We can speculate that kinetic effects and/or the action of the chelators on other biologically relevant metals and the susceptibility of the microorganism to withdrawal of these metals will also play a crucial role that remains to be studied. The coordination chemistry of the 1-hydroxy-2(1H)-pyridinone coordinating group in hexadentate ligands is still poorly studied. It is therefore not possible to make definitive judgements on the ability of these chelators to selectively bind Fe^{3+} in the presence of other biologically relevant metals such as Cu^{2+}, Mn^{2+}, Zn^{2+} (the amount of relevant metals in the growth medium was measured and found to be 65.7 μM for iron, 31.5 μM for zinc, 13.7 μM for manganese, 8.3 μM for cobalt and 4.5 μM for copper) and therefore how complexation of these biologically relevant metals could influence growth.

The measured stability constants for **34** and **35** indicate a strong preference of these HOPO derivatives for Fe^{3+} over Cu^{2+} and the higher concentration of iron in the medium suggest that the disruption of iron homeostasis is however a key factor influencing growth. However, the large difference in MIC between **3** and **9** for *K. pneumoniae* suggest that the positional isomerism may have a more subtle impact on

biological activity than expected from a simple inspection of the pKa and stability constants of the analogue coordinating groups **34** and **35**.

When comparing the general efficacy of each chelator (Table 3), it can be seen that TACN-MeHP, **1**, **3** and **6** are almost systematically the most effective. As TACN-MeHP is the most powerful Fe^{3+} chelator known, this is not a completely unexpected result. On the contrary, **8** and EMECAM, and to a lesser extend **9** are almost systematically the least effective compounds. It is interesting that EMECAM, known as a powerful Fe^{3+} chelator (pFe^{3+} = 32.6, compare with enterobactin: pFe^{3+} = 35.5 and with most natural siderophores having pFe^{3+} in the range 25-30[19]) is not a powerful biostatic agent against these microorganisms. This might be associated with some level of siderophore piracy because EMECAM is based on catechol coordinating groups, widely present in natural siderophores and it is known that synthetic chelators based on catechol groups can promote bacterial growth.[69-70] The addition of a benzo group on the HOPO (compare **1** and **3**) does not significantly alter the chelator's efficacy, except against *S. aureus*. We therefore suggest that the selection of hydroxypyridinone coordinating groups is a shrewd choice to achieve effective growth inhibition for a diverse range of microorganisms with little chance of growth promotion. The addition of a benzo group does not appear necessary to prevent siderophore piracy. It is interesting to note that the difference between the efficacious chelator **3** and the poor chelator **8** is only on the substitution of the amide nitrogen atom (H and CH_3 respectively). We have not yet measured the stability constants and pKa of the chelators, hence the effect of the methyl group on the thermodynamics of metal chelation is not known for these compounds. In the case of catechol-based or 3,2-HOPO-based hexadentate chelators, the addition of a methyl substituent on the nitrogen atom to remove the hydrogen bonding between the amide's N-H group and the coordinating atoms of the chelator did not significantly affect the Fe^{3+} stability constant of the compound.[71-73] The comparison of the efficacy of **3** (most efficacious) and its isomer **9** (poorer efficacy) indicates that the attachment on the linker onto the 1,2-HOPO group is also key to obtaining growth inhibition. Once again, this observation may be rationalised once the pKa and stability constants are measured. This shows that the study of a wide range of linker groups and an understanding of their effect on metal chelation, including thermodynamic and kinetic aspects are required to develop chelators for therapeutic applications.

Table 3. Ranking of chelator susceptibility (lowest MIC to highest MIC expressed in μM) for each microorganism

Microorganism	**Chelator Susceptibility**
E. coli DSM-18039	*TACN-MeHP > 3, 6 > 1, 7, 10 > 9, DTPA > EMECAM > 8*
K. pneumoniae DSM-30104	*3, TACN-MeHP > 6 > 1, 10 > EMECAM > 7, DTPA > 9 > 8*
P. aeruginosa DSM-19880	*1, 3, 6 > 7, 10, TACN-MeHP > EMECAM > 9 > DTPA > 8*
A. baumannii DSM-30007	*1 > TACN-MeHP > 3, 6, 7, 9, 10 > 8 > EMECAM > DTPA*
B. subtilis DSM-23778	*TACN-MeHP > DTPA > 3, 6, 9 > 1, 7, 8, 10 > EMECAM*
S. aureus DSM-1104	*3, 9 > DTPA, TACN-MeHP, 10 > 1, 6 > EMECAM > 7, 8*
C. albicans DSM-1386	*TACN-MeHP > 7 > 6, 8 > DTPA, 1, 3, 9 > 10 > EMECAM*

The growth of selected microorganisms with selected chelators over time, at different concentrations of compounds was followed be measurement of the optical density.

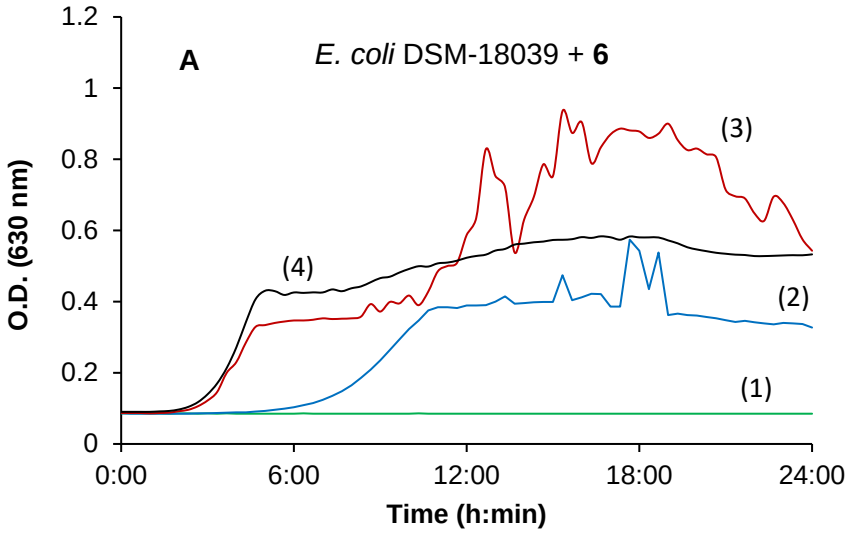

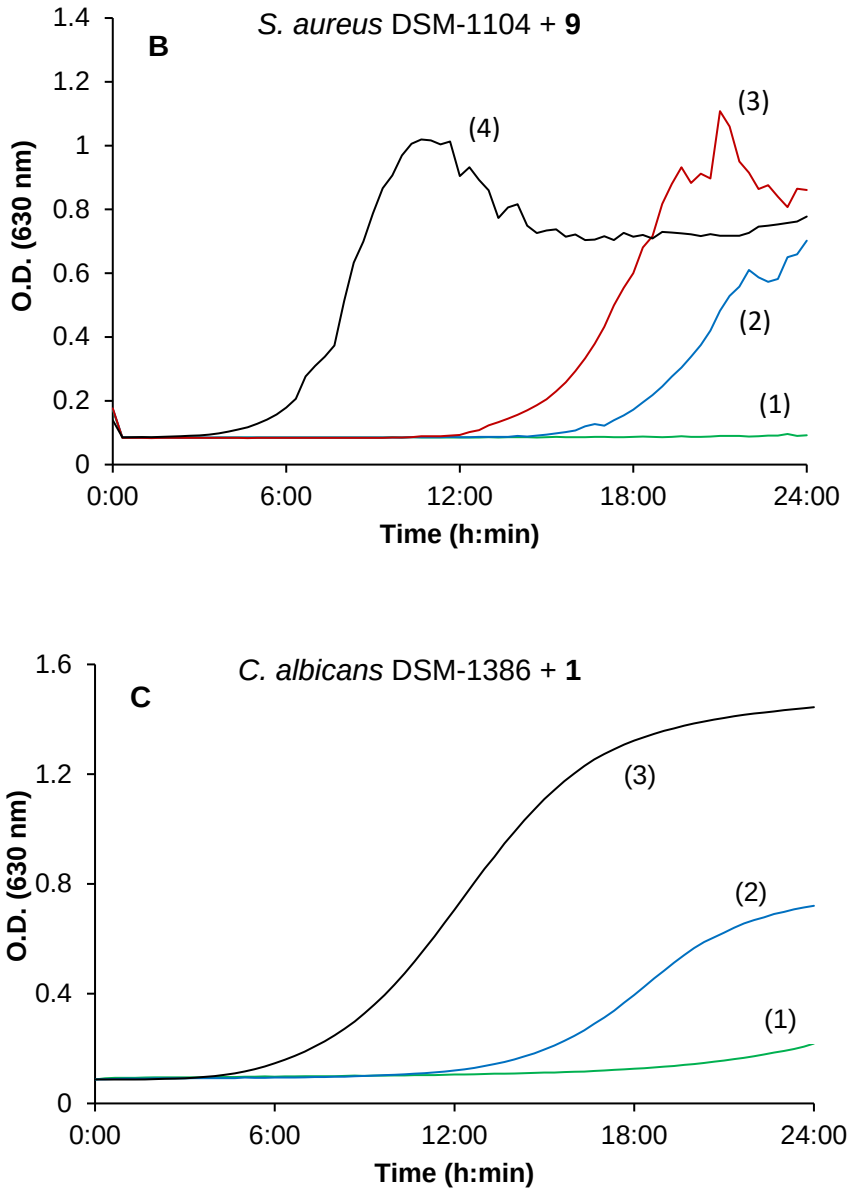

Figure 10. Impact of sub MIC concentrations on growth of selected microorganisms. Panel A describes *E. coli* DSM-18039 grown with **6**; Panels B described *S. aureus* DSM-1104 grown with 9 and panel C describes *C. albicans* DSM-1386 grown with **1**. concentrations: MIC (green, (1)) ; two sub-MIC concentrations MIC / 2 (blue, (2)), and the untreated control (black, (3)).

Each microorganism grew in the absence of chelator with clear lag and an exponential growth phases. In the presence of the chelators, the lag-phase generally appeared longer and was influenced by the concentration of chelator, the higher the concentration, the longer the lag-phase. To quantify the impact of

the chelator on the lag-phase, we expressed the duration of the lag-phase by the Growth Inhibition Factor (GIF) defined by equation 1:

$$GIF = \frac{t_c}{t_0} \quad \textbf{Equation 1}$$

where t_c is the duration of the lag phase in the presence of the chelator and t_0 is the duration of the lag-phase in the absence of the chelator (Table 4).

Table 4. Calculated Growth Inhibition Factors (GIF) for the apparent length of the lag phase of microbial growth at sub-MIC ligand concentrations over a period of 24 h. Positive controls for microbial growth were conducted in quadruplicate and the average reported.

Concentration	**Chelator**							$t_{0\ /\ min}$
	1	**3**	**6**	**7**	**8**	**9**	**10**	
E. coli DSM-18039								
MIC / 2	1.4	1	2.3	1.4	1.3	1.8	1.2	180
MIC / 4	1.4	1	1	1.1	1.1	1.4	1.2	
K. pneumoniae DSM-30104								
MIC / 2	2.4	1	1.9	2.3	+	3.6	1.4	140
MIC / 4	1.3	1	1	1.6	+	2	1.1	
P. aeruginosa DSM-19880								
MIC / 2	1.86	1.12	1.12	1.67	1.4	2.7	1.4	215
MIC / 4	1.12	1.02	1.12	1.21	1.3	1.95	1.12	
A. baumannii DSM-30007								
MIC / 2	1.64	1.13	1.33	1.44	2.36	1.13	1.95	195
MIC / 4	1.33	0.82	1.23	1.23	1.74	0.92	1.33	
B. subtilis DSM-23778								
MIC / 2	1.5	1.29	1.21	1	4.5	1.14	A	280
MIC / 4	N.R.	N.R.	1	N.R.	1.29	N.R.	A	
S. aureus DSM-1104								
MIC / 2	0.84	3.53	1.49	1.02	2.23	4.19	2.98	215
MIC / 4	1.02	1.86	1.12	N.R.	1.12	3.35	N.R.	
C. albicans DSM-1386								
MIC / 2	3.49	0.8	0.87	1.02	0.8	0.8	0.87	275
MIC / 4	2.47	X	0.87	1.02	0.87	0.8	3.78	

(+) Denotes no inhibition of growth was observed at the maximum concentration (5 mM) tested. 'A' denotes an ambiguous result due to ligand precipitation, 'N.R.' denotes that no result was taken (and 'X' that the sample failed to grow.

As can be seen, the extension of the lag-phase is dependent upon the concentration of chelator applied, which is wholly consistent with competition for a key nutrient. Until sufficient siderophores (and other metal acquisition mechanisms, if appropriate) are produced, the growth rate is severely reduced. Once the metal deprivation effect of the chelator is overwhelmed by the bacteria's own metal acquisition system, growth can resume. The higher the concentration of chelator, the longer it takes for the bacteria to overwhelm the chelator. Some results are, however, puzzling. For example, although *C. albicans* appeared quite susceptible to our chelators, the lag-phase generally does not always increase with chelator concentration. This might indicate a more complex mechanism of action with this fungus; the chelator could have a biocidal rather than biostatic effect. There does not seem to be any direct correlation between the GIF value and the MIC (Tables S4-S5). As mentioned before, the microorganisms that tend to show the lowest MIC value across the tested chelators are *C. albicans*, *S. aureus* and *B. subtilis* whereas the microorganisms that tend to show the largest GIF are *K. pneumoniae, S. aureus*. Similarly, whereas chelators TACN-MeHP, **1**, **3** and **6** were almost systematically the ones showing smallest MIC values, the chelators that show the largest GIF values are **1**, **8** and **9** (the GIF value for TACN-MeHP was not measured).

3- Conclusion

A range of novel secondary/tertiary amine/amide chelators based on 1,2-HOPO and the TREN core has been prepared and their antimicrobial effects evaluated upon a panel of microorganisms. Our results suggest that they indeed act as powerful metal chelators and likely inhibit bacterial growth by Fe^{3+} starvation. It would appear that both the nature of the linker (e.g. amide/amine), the attachment and the presence of additional substitution on the 1,2-HOPO have a large impact on the MIC values and these should be taken into consideration when designing therapeutic biostatic chelators. Further work is in progress to measure the Fe^{3+} stability constants and pKa of these hexadentate chelators to rationalise their biological function. Also, more investigations on their mode of action on microorganisms are in progress to gain a deeper understanding of their ability as biostatic agents against infection.

4- Experimental

4.1 Physical Measurements

Melting points were taken on a SRS DigiMelt MPA161 digital melting point apparatus with samples prepared in SAMCO soda glass capillary tubes 100mm. NMR spectra were recorded using a Jeol JNM Ex270 instrument at 270 MHz and 68 MHz or a Jeol JNM-ECS400 instrument at 400 MHz and 100 MHz, as specified, for ^{1}H- and ^{13}C- NMR respectively, and are reported in ppm (δ). Infrared spectra were obtained using Durascope diamond ATR system on a Perkin Elmer RX1 FTIR spectrometer. Positive and negative electrospray ionisation mass spectrometry (ESI-MS) was conducted using a Thermo LCQ Advantage mass spectrometer by direct injection and high resolution mass spectrometry (HRMS) was performed by the EPSRC National Mass Spectrometry Service (Swansea, Wales). UV-Visible spectrophotometry was conducted using a Varian Cary 50 UV-vis spectrophotometer (range 200 - 800 nm) using a 1 cm quartz cell at room temperature (18 - 22°C). Optical density readings were taken using a Biotek HT Multi-mode Microplate reader at the wavelength specified.

Physicochemical measurements

Water was purified by reverse osmosis followed by passaging through a mixed bed of ion-exchanger (R3 type; Thermo Fisher Scientific) and activated carbon (Oxygen Release Compound (ORC) type; Thermo Fisher Scientific). All stock solutions were prepared by weighing solid products using an analytical balance (precision 0.01 mg; AG245; Mettler Toledo). Metal cation solutions were prepared from their perchlorate salts. Their concentrations were determined via colorimetric titrations with EDTA (Titriplex III, Merck Millipore), in accordance with standard procedures[74-75] Sodium hydroxide and perchloric acid were used to adjust pH during titrations. The ionic strength of all solutions was fixed at 0.1 M with sodium perchlorate.

Potentiometry

The protonated forms of the ligands **34** and **35** and the stability constants (log *β*) of their complexes with Cu^{2+} were characterized by potentiometric titrations in water. Titrations were performed using an automatic titrator system (DMS 904 Titrino, Metrohm) with a combined glass electrode (Metrohm,

6.0234.100, Long Life) filled with NaCl 0.1 M. The electrode was calibrated as a hydrogen concentration probe by titrating known amounts of perchloric acid with CO_2 − free sodium hydroxide solutions. The GLEE program[76-77] was applied for the glass electrode calibration, and allowed to check the carbonate percentage in the NaOH solution used. In a typical experiment, an aliquot of 10 mL of ligand (10^{-3} M) or Cu:L (([L]/[Cu^{2+}] ≈ 2.2, L=**34** or **35**) was introduced into a thermostated jacketed cell (25.0(2) °C) and the solution was de-oxygenated by bubbling with oxygen-free argon. The titrations were then carried out by addition of known volumes of sodium hydroxide solution over the pH range 2–12. The Fe^{3+} complexes were already fully formed at pH 2 and could thus not be studied by this technique.

The potentiometric data were refined with the Hyperquad 2008 program[78] which uses non-linear least-squares methods, taking into account the formation of metal hydroxide species. The titration of each system was repeated in triplicate. The distribution curves as a function of pH of the protonated forms of **34**, **35** and their Cu^{2+} complexes were calculated using the Hyss2009 program.[79] The hydrolysis constants of Cu^{2+} at 25 °C and 0.1M ionic strength used in the calculations were taken from ref [80].

Spectrophotometry

The protonation constants of the ligands **34** and **35**, and their stability constants with Fe^{3+} were determined by UV-Visible spectrophotometric titrations versus pH, by recording simultaneously pH and UV-visible spectra. Between p[H] = −0.5 and p[H] = 2 (the brackets indicate that the pH value was calculated from the concentration of acid following p[H]=-log[H^+]), the batch technique was used following a previously published procedure.[81]

Between pH 2 and 12.5, continuous titrations were carried out. For the protonation studies, an aliquot of 30 mL of ligand **34** or **35** solution was introduced into a thermostated jacketed cell (25.0(2)°C). A known volume of perchloric acid solution was added to adjust the pH to ~2 and a dynamic titration was carried out by addition of known volumes of NaOH solution by a Metrohm 904 Titrino equipped with a 2 mL Dosino 800 burette driven by the Tiamo 2.5 software. The titrator was interfaced with an Agilent Cary 60

UV-Visible spectrophotometer which automatically recorded a spectrum after an equilibration time of 2 min following each addition of base. The complexation studies of ligands **34** and **35** with Fe^{3+} were carried out in the same way, on M:L (L = **34** or **35**) stoichiometric ratios $[L]/[Fe^{3+}] = 3.2$.

Titrations of ligands **34** and **35** by Fe^{3+} were also carried out at pH 2 in 0.01 M $HClO_4$ (I = 0.1M $NaClO_4$). 2.5 mL of ligand solution were transferred to a 1 cm quartz suprasil cuvette, aliquots of Fe^{3+} were added and an UV-Visible spectrum was recorded after each addition.

Competition experiments with EDTA in Hepes buffer at pH 7.4 were also carried out using the batch technique. Each batch sample contained an equivalent concentration of FeL_3 complex ($[L]/[Fe^{3+}]=3.2$, L=**34** or **35**) and increasing amounts of EDTA ($0<[EDTA]/[Fe^{3+}]<1$). The samples were left to equilibrate for the night before an UV-visible spectrum was recorded.

All the spectrophotometric data were fitted with Hypspec software[78] (http://www.hyperquad.co.uk), which allowed the calculation of the protonation constants of the ligands, the stability constants (log β) of the formed species and the coordination model of the studied systems. The hydrolysis constants of Fe^{3+} at 25 °C and 0.1 M ionic strength used in the calculations were taken from ref [80].

4.2 Synthesis

All solvents and reagents were purchased from Sigma-Aldrich, Acros Organics or Alfa-Aesar and used without further purification unless otherwise specified. Reactions were followed by TLC using silica gel with UV_{254} fluorescent indicator and column chromatography was conducted using 0.060 - 0.20 mm silica gel (70 - 230 mesh), where automated flash column chromatography was conducted using a Biotage Isolera One ISO-1SV. Hydrogenations performed using an H-cube® continuous flow hydrogen generator was operated as specified. Compound **1** was synthesised as described by K. N. Raymond (in 46% and 64% in the last two steps respectively).[55] Compound **3** was synthesised as described by K. N. Raymond (in 75% and 86% in the last two steps respectively).[52] Compounds **12** and **14** were synthesised as described by us.[48] Compounds **22** and **35** were synthesised as described by K. N. Raymond.[57, 82]

1-(Allyloxy)-6-(chloromethyl)-2(1H)-pyridinone (**15**). A solution of **12** (4.88 g, 27 mmol) in dichloromethane (120 mL) was added thionyl chloride (12 mL, 165 mmol) and refluxed for 6 h. Ice water (100 mL) was added at 0°C and stirred for 30 min. The phases were then separated and extracted with dichloromethane (2 × 100 mL). The combined organics were dried using magnesium sulfate, filtered and solvent removed *in vacuo*, yielding a brown oil which solidified upon standing (4.95 g, 92%); mp 62-65°C. δ_H (400 MHz; $CDCl_3$; Me_4Si) 4.57 (2H, s) 4.93 (2H, d, *J* 6.7 Hz) 5.47 (2H, m) 6.12 (1H, m) 6.25 (1H, dd, *J* 1.7, 6.7 Hz) 6.68 (1H, dd, *J* 1.7, 9.2 Hz) 7.27 (1H, dd, *J* 7.0, 9.4 Hz); δ_C (100 MHz) 39.5, 77.5 106.4, 122.5, 123.1, 130.3, 137.8, 144.3, 159.3; HRMS NESP: requires; m/z 200.0478, found; 200.0472 (M^+).

1-(Allyloxy)-2(1H)-pyridinone-6-carbaldehyde (**16**). To a 3 necked flask charged with oxalyl chloride (3.14 g, 40 mmol) in dichloromethane (30 mL) and lowered to - 60°C, dimethyl sulfoxide (4.14 g, 33 mmol) in dichloromethane (10 mL) was added dropwise over 5 min, and allowed to stir for 10 min. A solution of **12** (3.95 g, 20 mmol) in dichloromethane (100 mL) was then added dropwise over 5 min and stirred for an additional 2 h, before addition of triethylamine (10.98 g, 109 mmol) in dichloromethane (10 mL) over 5 min. The reaction was then allowed to reach ambient temperature at which point water (175 mL) was added, stirring for an additional 10 min. The 2 phases were separated, the aqueous phase extracted with dichloromethane (2 × 75 mL) and the combined organic phases were then washed with water (5 × 50 mL) before drying with magnesium sulfate, filtration and solvent removal *in vacuo*. Automated flash column chromatography of the crude (dichloromethane: methanol, 0-10%) yielded the product as a yellow oil, which solidified upon standing (1.15 g, 33%). The aldehyde was stored under nitrogen in the fridge as it was found to be susceptible to oxidation to the carboxylic acid upon standing at room temperature under air for a few months; mp 97-103°C. δ_H (400 MHz; $CDCl_3$; Me_4Si) 4.88 (2H, dd, *J* 6.9 Hz) 5.45 (2H, m) 6.81 (1H, dd, *J* 1.8, 6.9 Hz) 6.97 (1H, dd, *J* 1.8, 9.2 Hz) 7.44 (1H, dd, *J* 6.9, 9.2 Hz) 10.09 (1H, s); δ_C (100 MHz) 77.8, 108.5, 124.4, 129.2, 129.5, 137.2, 140.7, 158.0, 182.7; HRMS NESP: requires; m/z 180.0648, found; 180.0661 $(M-H)^+$.

Tris(N-[{1-allyloxy-2-oxo-1,2-dihydropyridin-6-yl}methyl]-2-aminoethyl)amine (**18**). A solution of aldehyde **16** (0.550 g, 3.1 mmol) in ethanol (20 mL) was added a solution of tris(2-aminoethyl)amine

(0.143 g, 0.98 mmol) in ethanol (5 mL) and stirred at reflux for 90 min. After cooling to 0°C, sodium borohydride (0.055 g, 1.5 mmol) was added portionwise and allowed to stir at room temperature for 16 h. The solution was then neutralised using concentrated hydrochloric acid (12 M) and the solvent removed *in vacuo*. Redissolution of the residue in aqueous sodium hydroxide (1 M; 50 mL) and extraction using dichloromethane (3 × 50 mL) followed by drying with magnesium sulfate, filtration and solvent removal *in vacuo* yielded a crude residue which was purified by automated flash chromatography (dichloromethane: methanol, 2-18%). The product was obtained as a viscous orange oil (0.098 g, 15%); R_f = 0.23 (dichloromethane: methanol, 9%). δ_H (400 MHz; $CDCl_3$; Me_4Si) 2.57 (6H, t, *J* 5.5 Hz) 2.65 (6H, t, *J* 5.5 Hz) 3.81 (6H, s) 4.81 (6H, d, *J* 6.4 Hz) 5.41 (6H, m) 6.05 (3H, m) 6.13 (3H, d, *J* 6.4 Hz) 6.56 (3H, dd, *J* 1.4, 9.2 Hz) 7.24 (3H, dd, *J* 6.9, 9.2 Hz); δ_C (100 MHz) 29.8, 46.6, 48.7, 54.2, 104.4, 120.6, 122.4, 130.4, 138.1, 147.5, 159.5.

Tris(N-[{1-hydroxy-2-oxo-1,2-dihydropyridin-6-yl}methyl]-2-aminoethyl)amine (**6**). Under an atmosphere of nitrogen, a solution of **18** (0.089 g, 0.14 mmol) in dry dichloromethane (5 mL) at 0°C was added boron trichloride in tetrahydrofuran (1.0 M; 0.98 mL, 0.98 mmol) and vigorously stirred overnight before the mixture was added methanol (2 mL) and stirred for 30 min further. The solution was then evaporated *in vacuo* and re-evaporated with methanol (5 mL) 5 times, yielding the crude product as brown flakes. Dissolution in a minimum volume of methanol and precipitation using diethyl ether yielding a light brown solid which was collected by Büchner filtration and washed with diethyl ether (0.054 g, 75%); mp 162-168°C (decomp.). δ_H (400 MHz; [D_6]-DMSO; Me_4Si) 2.85 (6H, t, br) 3.30 (6H, t, br) 4.36 (6H, s) 6.60 (3H, dd, *J* 1.4, 9.2 Hz) 6.64 (3H, dd, *J* 1.4, 7.3 Hz) 7.43 (3H, dd, *J* 7.3, 9.2 Hz) 9.58 (3H, s, br); δ_C (100 MHz) 44.4, 44.9, 49.3, 107.1, 119.4, 136.8, 138.4, 157.7; (+)-ESI-MS: m/z 516.16 ($M+H^+$); HRMS NESN: requires; 514.2414, found; 514.2405 $(M-H)^-$.

Tris(N-ethoxycarbonyl-2-aminoethyl)amine (**19**). Product was prepared as previously described.[51] (6.42 g, 92% (crude)). δ_H (400 MHz; $CDCl_3$; Me_4Si) 1.24 (9H, t, *J* 6.9 Hz) 2.56 (6H, m) 3.23 (6H, m) 4.13 (6H, q, *J* 6.9 Hz); δ_C (100 MHz) 14.7, 38.7, 53.8, 60.8, 157.3.

Tris(N-methyl-2-aminoethyl)amine (**20**). Product was prepared as previously described.[51] δ_H (400 MHz; $CDCl_3$; Me_4Si) 2.42 (9H, s) 2.58 (12H, m); δ_C (100 MHz) 36.6, 49.9, 54.4.

Tris(N-[{1-allyoxy-2-oxo-1,2-dihydropyridin-6-yl}methyl]-N-methyl-2-aminoethyl)amine (**21**). A mixture of **15** (0.600 g, 3.0 mmol) and potassium carbonate (0.872 g, 6.3 mmol) in acetonitrile (25 mL) was added **20** (0.189 g, 0.8 mmol) and stirred at reflux for 16 h. The resulting mixture was cooled to room temperature, filtered and the liquid filtrate removed *in vacuo*, yielding a thick brown residue which was purified by automated flash chromatography. The product was obtained as a glassy brown solid (0.240 g, 35%); R_f = 0.05 (dichloromethane: methanol, 5%). δ_H (400 MHz; $CDCl_3$; Me_4Si) 2.27 (9H, s) 2.54 (12H, m) 3.54 (6H, s) 4.83 (6H, d, *J* 6.4 Hz) 5.40 (6H, m) 6.07 (3H, m) 6.17 (3H, dd, *J* 1.8, 6.9 Hz) 6.56 (3H, dd, *J* 1.8, 9.2 Hz) 7.23 (3H, dd, *J* 6.9, 9.2 Hz); δ_C (100 MHz) 43.1, 55.9, 57.0, 105.0, 120.5, 121.6, 130.8, 137.9, 147.1, 159.8; (+)-ESI-MS: m/z 678.11 ($M+H^+$); HRMS NESP: requires; m/z 678.3979, found; 678.3979 ($M+H^+$).

Tris(N-[{1-hydroxy-2-oxo-1,2-dihydropyridin-6-yl}methyl]-N-methyl-2-aminoethyl)amine (**7**). A solution of **21** (0.158 g, 0.28 mmol) in a mixture of 1,4-dioxane and water (3: 1; 4 mL) was added 10% Pd/C (0.016 g) and trifluoroacetic acid (0.17 M; 0.156 g, 1.37 mmol) before stirring at reflux overnight. Upon cooling, filtration of the solid and solvent evaporation *in vacuo* yielded a viscous golden oil which was dissolved in a minimum volume of methanol and precipitated using diethyl ether, collecting the tan solid by Büchner filtration, rinsing with diethyl ether (0.103 g, 66%); mp 80°C. δ_H (400 MHz; [D6]-DMSO; Me_4Si) 2.71 (9H, s) 2.96 (6H, t, br) 3.27 (6H, t, br) 4.39 (6H, s) 6.57 (3H, dd, *J* 1.4, 6.9 Hz) 6.64 (3H, dd, *J* 1.4, 8.7 Hz) 7.42 (3H, dd, *J* 6.9, 8.5 Hz); δ_C (100 MHz) 41.3, 48.1, 53.4, 54.5, 109.0, 115.6, 118.6, 120.3, 137.0, 138.5, 158.6, 158.8, 159.1, 158.5, 159.5; (+)-ESI-MS: m/z 558.11 ($M+H^+$); HRMS NESP: requires; m/z 558.3040, found; 558.3034 ($M+H^+$).

Pentafluorophenyl 1-benzyloxy-2(1H)-pyridinone-6-carboxylate (**23**). A solution of **22** (0.40 g, 1.6 mmol) in dry N,N-dimethylformamide (4 mL) was added dropwise to a solution of pentafluorophenyl trifluoroacetate (0.59 g, 2.1 mmol) and pyridine (0.14 g, 1.8 mmol) in dry N,N-dimethylformamide at 0°C,

before stirring at ambient temperature for 1.5 h. The mixture was then diluted with ethyl acetate (300 mL) and washed with aqueous hydrochloric acid (0.1 M; 3 × 50 mL), aqueous sodium hydrogen carbonate (5%; 3 × 50 mL) and brine (50 mL) before drying the organics with magnesium sulfate, filtration and solvent removal *in vacuo* to yield the crude product as a crystalline cream solid was used without purification. δ_H (400 MHz; $CDCl_3$; Me_4Si) 5.41 (2H, s) 6.96 (1H, dd, *J* 1.8, 6.9 Hz) 7.01 (1H, dd, *J* 1.4, 9.2 Hz) 7.35-7.39 (3H, m) 7.42 (1H, dd, *J* 6.9, 9.2 Hz) 7.52-7.54 (2H, m); δ_C (100 MHz) 78.9, 111.4, 124.2 (m), 128.6, 129.4, 130.2, 133.1, 135.2, 136.9 (m), 137.0, 138.8 (m), 139.3 (m), 139.9 (m), 141.4 (m), 142.4 (m), 155.2, 158.9, 162.9; (+)-ESI-MS: m/z 433.89 ($M+Na^+$).

Tris(N-[1-benzyloxy-2-oxo-1,2-dihydropyridine-6-carbonyl]-N-methyl-2-aminoethyl)amine (**24**). A solution of N,N-diisopropylethylamine (0.63 g; 4.9 mmol) and **20** (0.13 g, 0.7 mmol) in N,N-dimethylformamide (10 mL) at 0°C was added **23** (1.10 g; 2.7 mmol) in N,N-dimethylformamide (12 mL) dropwise before being allowed to warm to ambient temperature and subsequently stirred overnight. The solution was then concentrated to dryness *in vacuo* and the resulting residue dissolved in dichloromethane (100 mL), washed with saturated aqueous sodium hydrogen carbonate (3 × 100 mL), water (100 mL) and brine (100 mL) before drying using magnesium sulfate, filtration and solvent removal *in vacuo*. The crude product was purified using automated flash column chromatography (dichloromethane: methanol, 1-12%). Evaporation of the solvent yielded the purified product as an opaque oil (0.35 g, 58%). δ_H (400 MHz; $CDCl_3$; Me_4Si) 1.81-3.42 (20H, m) 4.00 (1H, t, *J* 6.0 Hz) 4.93-5.05 (3H, m) 5.39-5.60 (3H, m) 5.96-6.08 (3H, m) 6.57-6.74 (3H, m) 7.31-7.38 (12H, m) 7.46-7.54 (6H, m); δ_C (100 MHz) 26.96, 33.2, 77.2, 79.2, 79.2, 79.5, 102.6, 102.9, 102.9, 122.7, 123.1, 128.5, 129.3, 129.5, 129.5, 130.1, 130.2, 130.2, 130.5, 130.5, 133.4, 133.6, 138.3, 138.5, 142.8, 143.0, 143.1, 158.1, 158.3, 158.3, 161.7, 161.8, 161.9; (+)-ESI-MS: m/z 892.08 ($M+Na^+$) 870.08 ($M+H^+$); HRMS NESP: requires; m/z 870.3827, found; 870.3830 ($M+H^+$).

Tris(N-[1-hydroxy-2-oxo-1,2-dihydropyridine-6-carbonyl]-N-methyl-2-aminoethyl)amine (**8**). A solution of **24** (0.350 g; 0.4 mmol) in a mixture of concentrated hydrochloric acid and glacial acetic acid (1:1; 20 mL) was stirred at room temperature for 3 days then for 16 h at 50°C before solvent removal *in*

vacuo to yield a white 'foamy' solid as crude product. The crude solid was then dissolved in a minimum amount of methanol and precipitated with diethyl ether, yielding a white solid (0.218 g, 90%); mp 140-142°C. δ_H (400 MHz; [D_6]-DMSO; Me_4Si) 2.78-3.92 (21H, m) 6.14-6.41 (3H, m) 6.56 (3H, m) 7.37-7.45 (3H, m); δ_C (100 MHz) 32.8, 36.3, 41.7, 103.1, 120.1, 138.4, 141.9, 158.0, 162.6; (+)-ESI-MS: m/z 653.01 ($FeM+H^+$); HRMS NESN: requires; m/z 598.2261, found; 598.2261 $(M-H)^-$.

1-Benzyloxy-2(1H)-pyridinone-3-carboxylic acid (**25**). A mixture of **14** (3.52 g, 23 mmol), potassium carbonate (5.53 g, 40 mmol) and benzyl bromide (4.05 g, 24 mmol) was refluxed in methanol (110 mL) for 16 h before solvent removal *in vacuo*. The residue was then taken into a biphasic mixture of water and diethyl ether (1:1; 240 mL) and acidified using aqueous hydrochloric acid (6 M; pH 1) causing precipitation of the product as an off white solid. Drying of the solid *in vacuo* over phosphorus pentoxide yielded a white powder (4.73 g, 85%); mp 167-169°C. δ_H (400 MHz; [D_6]-DMSO; Me_4Si) 5.32 (2H, s) 6.59 (1H, t, *J* 7.1 Hz) 7.42-7.54 (5H, m) 8.33 (2H, m); δ_C (100 MHz) 79.7, 107.3, 119.8, 129.2, 130.0, 130.6, 133.7, 143.4, 144.8, 160.3, 164.8; (+)-ESI-MS: m/z 267.94 ($M+Na^+$), 245.92 ($M+H^+$); HRMS NESP: requires; m/z 268.0586, 246.0766, found; 268.0585 ($M+Na^+$), 246.0765 ($M+H^+$).

1-Benzyloxy-1,2-dihydro-2-oxo-3-([2-sulfanylidene-1,3-thiazolidin-3-yl]carbonyl)pyridine (**26**). A mixture of **25** (2.15 g, 9 mmol), 1-ethyl-3-(3-dimethylaminopropyl)carbodiimide hydrochloride (5.48 g, 29 mmol) and 2-mercaptothiazoline (1.13 g, 10 mmol) in dry dichloromethane (40 mL) was added a catalytic quantity of 4-dimethylaminopyridine and stirred overnight at room temperature. The solution was then washed with aqueous hydrochloric acid (1 M; 2 × 50 mL), aqueous sodium hydroxide (1 M; 2 × 50 mL) and brine (50 mL) before drying over magnesium sulfate, filtration and solvent removal *in vacuo* to yield a bright yellow gum (1.41 g, 44%). δ_H (400 MHz; $CDCl_3$; Me_4Si) 3.48 (2H, t, *J* 7.3 Hz) 4.61 (2H, t, *J* 7.3 Hz) 5.19 (2H, s) 5.98 (1H, t, *J* 7.1 Hz) 7.16 (1H, dd, *J* 1.8, 6.9 Hz) 7.35-7.40 (5H, m) 7.54 (1H, dd, *J* 1.8, 6.9 Hz); δ_C (100 MHz) 29.7, 56.0, 78.5, 104.0, 128.9, 129.5, 130.4, 133.6, 139.9, 140.5, 155.7, 166.3, 202.5; (+)-ESI-MS: m/z 368.94 ($M+Na^+$); HRMS NESP: requires; m/z 369.0343, 347.0524, found; 369.0342 ($M+Na^+$), 347.0524 ($M+H^+$).

Tris(N-[1-benzyloxy-2-oxo-1,2-dihydropyridine-3-carbonyl]-2-aminoethyl)amine (**27**). A solution of **26** (1.41 g, 4.1 mmol) in dry dichloromethane (40 mL) was added TREN (0.17 g, 1.1 mmol) dropwise and stirred at room temperature overnight. The solvent was then removed *in vacuo* and the residue purified by column chromatography (dichloromethane: methanol, 0 - 5%). The product was obtained as a yellow gum (0.95 g, 88%); R_f = 0.34 (dichloromethane: methanol, 5%). δ_H (400 MHz; $CDCl_3$; Me_4Si) 2.93 (6H, t, *J* 6.6 Hz) 3.64 (6H, q, *J* 6.3 Hz) 5.25 (6H, s) 6.07 (3H, t, *J* 7.1 Hz) 7.23 (3H, dd, *J* 2.3, 6.9 Hz) 7.34-7.39 (5H, m) 8.39 (*J* 2.3, 7.3 Hz) 9.76 (3H, t, *J* 5.5 Hz); (+)-ESI-MS: m/z 828.12 ($M+H^+$), + p FTMS NSI: requires; m/z 828.3357, found; 828.3351 ($M+H^+$).

Tris(N-[1-hydroxy-2-oxo-1,2-dihydropyridine-3-carbonyl]-2-aminoethyl)amine (**9**). A solution of **27** (0.85 g, 1.0 mmol) in concentrated hydrochloric acid (10 mL) and glacial acetic acid (10 mL) was stirred at 50°C for 4 days. The solvent was then removed *in vacuo*, yielding the product as a crude brown foam. Trituration of the solid in methanol yielded pure product as a tan solid which was collected by Büchner filtration and washed with diethyl ether. Precipitation from the mother liquor by diethyl ether addition yielded further product as a brown solid (0.44 g, 82%); mp 160-164°C. δ_H (400 MHz; $[D_6]$-DMSO; Me_4Si) 3.42 (6H, t, br) 3.75 (6H, q, *J* 6.0 Hz) 6.43 (3H, t, *J* 7.1 Hz) 8.12 (3H, dd, *J* 1.8, 7.3 Hz) 8.27 (3H, dd, *J* 2.3, 6.9 Hz) 9.77 (3H, t, *J* 6.0 Hz); δ_C (100 MHz) 34.5, 52.8, 105.1, 120.2, 140.5, 141.1, 158.4, 164.7; (+)-ESI-MS: m/z 580.18 ($M+Na^+$), 558.08 ($M+H^+$); HRMS NESP: requires; m/z 580.1768, 558.1949, found; 580.1754 ($M+Na^+$), 558.1938 ($M+H^+$).

1-Hydroxy-2-oxo-1,2-dihydroquinoline-3-carboxylic acid (**28**). The corresponding ethyl ester (1.34 g, 5.75 mmol) was stirred at room temperature for 1 h in the presence of 2.82 g of sodium hydroxide (70.5 mmol) and 15 mL of water, upon which a yellow solid precipitated. After cooling in ice, the solution was made acidic with concentrated hydrochloric acid. The yellow solid first resolubilised (while the solution was still alkaline) then a white solid precipitated once acidic. It was filtered, rinsed with cold water and recrystallized in ethanol/water (0.95 g, 81%). δ_H (400 MHz; $[D_6]$-DMSO; Me_4Si) 8.87 (1H, s) 8.07 (1H, d) 7.88-7.78 (2H, m), 7.42 (1H, dt); δ_C (100 MHz) 113.7, 118.7, 118.8, 124.6, 131.2, 135.0, 140.1, 143.4, 159.6, 164.8; (+)-ESI-MS: m/z 227.97 ($M+Na^+$); (-)-ESI-MS: m/z 204.05 ($M-H^+$).

1-Benzyloxy-2-oxo-1,2-dihydroquinoline-3-carboxylic acid (**29**). A suspension of **28** (2.00 g, 10 mmol) and potassium carbonate (2.69 g, 19 mmol) in methanol (130 mL) was added benzyl bromide (1.67 g, 10 mmol) and refluxed for 24 h. The mixture was concentrated to dryness before resuspension in a mixture of water (175 mL) and diethyl ether (75 mL), which was then acidified, under stirring at 0°C, using aqueous hydrochloric acid (4 M; pH 2). The resulting precipitate was collected by Büchner filtration and washed liberally with water before drying *in vacuo* over phosphorus pentoxide. The product was obtained as a white solid (2.38 g, 83%); mp 202-203°C. δ_H (400 MHz; [D_6]-DMSO; Me_4Si) 5.23 (2H, s) 7.39 (4H, m) 7.59 (2H, m) 7.67 (1H, d, *J* 8.2 Hz) 7.81 (1H, t, *J* 7.8 Hz) 8.04 (1H, d, *J* 7.8 Hz) 8.83 (1H, s); δ_C (100 MHz) 77.9, 113.1, 118.9, 120.5, 124.8, 129.2, 129.9, 130.6, 131.4, 134.0, 135.1, 139.4, 144.4, 158.8, 164.8; (+)-ESI-MS: m/z 317.99 ($M+Na^+$); HRMS NESP: requires; m/z 318.0742, 296.0923, found; 318.0741 ($M+Na^+$), 296.0922 ($M+H^+$).

1-Benzyloxy-2-oxo-1,2-dihydroquinoline-3-carbonyl chloride (**30**). A mixture of **29** (1.78 g, 6 mmol) in toluene (50 mL) was added oxalyl chloride (2.1 mL, 25 mmol) and a catalytic quantity of N,N-dimethylformamide (2 drops) before raising the temperature to 40°C for 4 h. The solution was then concentrated in vacuum and co-evaporated with toluene (20 mL). The solid was re-suspended in toluene (20 mL), filtered and solvent again removed *in vacuo*, yielding the crude product as a bright yellow solid which was used without further purification (1.16 g, 51%); mp 159-166°C. δ_H (400 MHz; $CDCl_3$; Me_4Si) 5.28 (2H, s) 7.35 (1H, m) 7.39-7.44 (3H, m) 7.58-7.63 (3H, m) 7.73-7.79 (2H, m) 8.80 (1H, s); δ_C (100 MHz) 77.6, 112.6, 116.9, 123.8, 124.8, 128.7, 129.5, 130.0, 130.1, 131.0, 133.3, 135.6, 140.6, 148.3, 161.9; (+)-ESI-MS: m/z 331.98 ($M(+MeOH-HCl)+Na^+$).

Tris(N-[1-benzyloxy-2-oxo-1,2-dihydroquinoline-3-carbonyl]-2-aminoethyl)amine (**31**). A solution of **30** (1.06 g, 3.4 mmol) in toluene (40 mL) was added dropwise at 0°C to a solution of triethylamine (0.51 g, 5.0 mmol) and tris(2-aminoethyl)amine (0.15 g, 1.0 mmol) in toluene (10 mL). The mixture was then raised to room temperature and stirred. After 4 days, the mixture was partitioned between ethyl acetate (50 mL) and saturated aqueous sodium hydrogen carbonate (50 mL) and separated, forming a thick

emulsion. Following separation, dichloromethane (3 × 50 mL) was used to extract the remaining organics from the aqueous phase before combination of the organics and drying using magnesium sulphate, filtration and solvent removal *in vacuo*. The crude residue was purified by column chromatography (dichloromethane: methanol, 0-4%), obtaining the product as a pale yellow solid (0.65 g, 65%); mp 222-224°C. δ_H (400 MHz; $CDCl_3$; Me_4Si) 2.99 (6H, t, *J* 6.2 Hz) 3.72 (6H, q, *J* 5.8 Hz) 5.10 (6H, s) 7.23 (3H, t, *J* 7.3 Hz) 7.27-7.32 (8H, m) 7.36-7.43 (10H, m) 7.55 (3H, m) 7.60 (3H, d, *J* 7.8 Hz) 8.72 (3H, s) 9.87 (3H, t, *J* 5.3 Hz); δ_C (100 MHz) 38.6, 53.7, 77.4, 112.2, 118.4, 122.9, 123.2, 128.6, 129.1, 129.7, 130.1, 132.6, 133.6, 139.0, 142.0, 157.9, 163.0; (+)-ESI-MS: m/z 978.16 ($M+H^+$); HRMS NESP: requires; m/z 978.3827, found; 978.3817 ($M+H^+$).

Tris(N-[1-hydroxy-2-oxo-1,2dihydroquinolin-3-carbonyl]-2-aminoethyl)amine (**10**). A solution of **31** (0.347 g, 0.35 mmol) in a concentrated hydrochloric acid: glacial acetic acid mixture (1: 1; 20 mL) was stirred for 4 days at 50°C, before solvent removal *in vacuo* to yield a white solid (0.150 g, 57%); mp 247-250°C. δ_H (400 MHz; [D_6]-DMSO; Me_4Si) 3.61 (6H, t, br) 3.85 (6H, q, br) 7.24 (3H, t, *J* 7.8 Hz) 7.60-7.74 (9H, m) 8.54 (3H, s) 9.92 (3H, t, *J* 5.5 Hz); δ_C (100 MHz) 34.8, 53.3, 113.1, 117.9, 121.3, 123.6, 130.5, 133.9, 139.7, 141.2, 157.8, 164.5; (+)-ESI-MS: m/z 708.08 ($M+H^+$); HRMS NESP: requires; m/z 708.2418, found; 708.2403 ($M+H^+$).

Tris(N-[N-oxy-pyridin-2-ylcarbonyl]-2-aminoethyl)amine (**32**). A solution of picolinic acid *N*-oxide (0.50 g, 3.6 mmol) in dry dichloromethane (30 mL) was added 1-ethyl-3-(3-dimethylaminopropyl)carbodiimide hydrochloride (0.69 g, 3.6 mmol) and triethylamine (1.25 mL, 9.0 mmol) at 0°C, stirring for 30 min. Tris(2-aminoethyl)amine (0.18 g, 1.2 mmol) was then added and the solution was stirred for 2 days at ambient temperature before extraction with aqueous hydrochloric acid (1M; 30 mL) and the organic phase discarded. Saturated aqueous sodium hydrogen carbonate (80 mL) was added to the aqueous phase and re-extracted with dichloromethane (3 × 50 mL) which was dried using sodium sulfate, filtered and the solvent removed *in vacuo*, yielding a crystalline brown solid (0.20 g, 32%); mp 145 - 152°C. δ_H (400 MHz; $CDCl_3$; Me_4Si) 2.91 (6H, t, *J* 6.4 Hz) 3.63 (6H, q, *J* 6.4 Hz) 7.31 (3H, td, *J* 2.3, 6.9 Hz) 7.40 (3H, dd, *J* 1.4, 8.2 Hz) 8.12 (3H, d, *J* 6.4 Hz) 8.37 (3H, dd, 1.8, 7.8 Hz) 11.33 (3H, t, br); δ_C (100 MHz) 38.3, 53.3, 126.6,

126.9, 128.7, 140.5, 140.9, 159.8; (+)-ESI-MS: m/z 532.21 ($M+Na^+$) 510.16 ($M+H^+$); HRMS NESP: requires 532.1921; m/z found; 532.1906 ($M+Na^+$) 510.2089 ($M+H^+$).

Tris(N-[2-hydroxypyridin-3-yl-carbonyl]-2-aminoethyl)amine (**33**). A mixture of 2-hydroxynicotinic acid (0.50 g, 3.6 mmol), triphenyl phosphine (1.01 g, 3.9 mmol), 2,2'-dipyridyl disulfide (0.85 g, 3.9 mmol) and tris(2-aminoethyl)amine (0.16 g, 1.1 mmol) in dry acetonitrile (25 mL) was stirred stoppered at 60°C for 48 h before the mixture was concentrated to dryness *in vacuo*. The resulting residue was suspended in methanol (25 mL) and refluxed for 30 min before cooling to 0°C and the obtained precipitate collected by Büchner filtration. The product was obtained as a white powder (0.19 g, 34%); mp > 260°C. δ_H (400 MHz; [D_6]-DMSO; Me_4Si) 2.70 (6H, t, br) 3.39 (6H, q, *J* 5.0 Hz) 6.44 (3H, t, *J* 6.4 Hz) 7.66 (3H, d, *J* 4.6 Hz) 8.29 (3H, d, *J* 6.0 Hz) 9.80 (3H, t, br) 12.40 (3H, s); δ_C (100 MHz) 37.2, 53.2, 105.9, 120.4, 139.0, 143.6, 162.1, 163.1; HRMS NESP: requires 532.1921; m/z found; 532.1906 ($M+Na^+$) 510.2089 ($M+H^+$).

1-Benzyloxy-N,N-dimethyl-2-oxo-1,2-dihydropyridine-3-carboxamide. A stirred suspension of 1-Benzyloxy-pyridin-2-one-3-carboxylic acid **24** (0.65 g, 2.7 mmol) and oxalyl chloride (0.40 g, 3.2 mmol) in toluene (10 mL) was added a catalytic amount of N,N-dimethylformamide (1 drop) before raising the temperature to 40 °C and stirring for 4 h. A solution of dimethylamine in tetrahydrofuran (2 M; 6 mL) was then added to the mixture of which was not isolated, causing dissolution. Following overnight stirring, the solvent was removed under high vacuum before the residue was taken up into aqueous sodium hydroxide (1 M; 30 mL) and extracted with dichloromethane (3 × 30 mL). The combined organics were then washed with aqueous hydrochloric acid (1 M; 100 mL) and brine (100 mL) before drying with magnesium sulfate, filtration and solvent removal *in vacuo* yielding the product as an orange oil (0.51 g, 71%). δ_H (400 MHz; $CDCl_3$; Me_4Si) 3.00 (3H, s) 3.12 (3H, s) 5.29 (2H, s) 6.05 (1H, t, *J* 6.9 Hz) 7.28 (1H, dd, *J* 2.3, 7.3 Hz) 7.38-7.44 (5H, m) 7.50 (1H, dd, *J* 2.3, 6.9 Hz); δ_C (100 MHz) 35.2, 38.2, 78.8, 104.2, 128.8, 129.5, 130.2, 131.1, 133.3, 137.8, 138.7, 155.5, 166.5; (+)-ESI-MS: m/z 295.01 ($M+Na^+$); HRMS NESP: requires; m/z 273.1239, found; 273.1237 ($M+H^+$).

1-Hydroxy-N,N-dimethyl-2-oxo-1,2-dihydropyridine-3-carboxamide (**34**). A solution of 1-benzyloxy-N,N-dimethyl-pyridin-2-one-3-carboxamide (0.515 g, 1.9 mmol) in ethanol (20 mL) and water (5 mL) was acidified to pH 1 using concentrated hydrochloric acid before addition of Pd/C (10%; 0.051 g). Hydrogen gas was then bubbled through the mixture and the reaction stirred for 3 h at ambient temperature. The mixture was then filtered and the solvent removed *in vacuo* to yield an orange oil (0.320 g, 94%). δ_H (400 MHz; [D_6]-DMSO; Me_4Si) 2.83 (3H, s) 2.94 (3H, s) 6.26 (3H, t, *J* 6.9 Hz) 7.41 (1H, dd, *J* 2.3, 7.3 Hz) 8.00 (1H, dd, 2.3, 6.9 Hz); δ_C (100 MHz) 34.8, 37.9, 56.5, 104.4, 128.6, 137.0, 137.3, 155.4, 166.8; (+)-ESI-MS: m/z 205.00 ($M+Na^+$); HRMS NESP: requires; m/z 183.0770, found; 183.0763 ($M+H^+$).

4.3 Preparation of Stock Solutions

Glassware was rinsed with a deionised aqueous solution of EDTA (0.1 M) then rinsed thoroughly with deionised water (18 mΩ) before ligands were dissolved in deionised water to the desired concentration (5 mM; 5 mL). The stock solution was then passed through a membrane filter (0.22 µM) into a sterile bijoux tube (7 mL) and stored at 4°C until required.

4.4 Bacterial Strains

All strains were purchased from DSMZ. *E. coli* 18039, *K. pneumoniae* 30104, *P. aeruginosa* 19880 and *S. aureus* 1104 were cultured onto brain heart infusion (BHI) agar and incubated at 37°C for 24 h. Similar procedures were conducted for strains of *A. baumannii* 30007 and *C. albicans* 1386 incubated at 30°C and *B. subtilis* incubated at 25°C, all for 48 h. The cultured plates were then stored at 4°C until needed.

4.5 Antimicrobial Assay

Assay was conducted upon a similar literature procedure.[19] Stock solutions of ligands (5,000 µM) were added to the first wells of a 96 well-microtitre plate (200 µL) and sterile BHI broth (100 µL) was added to the remaining wells in the row. Ligand solution from the first well (100 µL) was added to the next well in the row and mixed. The procedure was then repeated along the row from the dilute solutions and discarded after the penultimate well. Inoculum (10^5 CFU/mL; 100 µL) was then added to all wells and the plate incubated without agitation at 37°C. Readings were taken after for 24 and 48 h, depending upon the

microorganism, and the MIC determined on the basis of visual turbidity of the well. Assays were performed in triplicate.

5- Declaration of Interest

None.

6- Acknowledgement

The authors are grateful for financial support from the Healthcare Infection Society (www.his.org.uk) and Northumbria University. The authors are also grateful for the support offered by the EPSRC National Mass Spectrometry Service (Swansea, Wales, UK) for high resolution mass spectrometry. Dr Frank Lewis (Northumbria University) and Dr Valery Kozhevnikov (Northumbria University) are also acknowledged for fruitful discussions.

7- References

1. Foley, T. L.; Simeonov, A., Targeting iron assimilation to develop new antibacterials. *Expert Opin. Drug Discov.* **2012,** *7* (9), 831-47.
2. Corbin, B. D.; Seeley, E. H.; Raab, A.; Feldmann, J.; Miller, M. R.; Torres, V. J.; Anderson, K. L.; Dattilo, B. M.; Dunman, P. M.; Gerads, R.; Caprioli, R. M.; Nacken, W.; Chazin, W. J.; Skaar, E. P., Metal chelation and inhibition of bacterial growth in tissue abscesses. *Science* **2008,** *319* (5865), 962-965.
3. Zhang, Y.; Ballard, E. C.; Zheng, S. L.; Gao, X.; Ko, K. C.; Yang, H.; Brandt, G.; Lou, X.; Tai, P. C.; Lu, C. D.; Wang, B., Design, synthesis, and evaluation of efflux substrate-metal chelator conjugates as potential antimicrobial agents. *Bioorg. Med. Chem. Lett.* **2007,** *17* (3), 707-11.
4. Thompson, M. G.; Corey, B. W.; Si, Y.; Craft, D. W.; Zurawski, D. V., Antibacterial activities of iron chelators against common nosocomial pathogens. *Antimicrob. Agents Chemother.* **2012,** *56* (10), 5419-21.
5. Zhou, T.; Winkelmann, G.; Dai, Z. Y.; Hider, R. C., Design of clinically useful macromolecular iron chelators. *J. Pharm. Pharmacol.* **2011,** *63* (7), 893-903.
6. Visca, P.; Bonchi, C.; Minandri, F.; Frangipani, E.; Imperi, F., The Dual Personality of Iron Chelators: Growth Inhibitors or Promoters? *Antimicrob. Agents Chemother.* **2013,** *57* (5), 2432-2433.
7. Nairz, M.; Schroll, A.; Sonnweber, T.; Weiss, G., The struggle for iron - a metal at the host-pathogen interface. *Cell. Microbiol.* **2010,** *12* (12), 1691-702.
8. Ratledge, C., Iron metabolism and infection. *Food Nutr. Bull.* **2007,** *28* (4 Suppl), S515-23.

9. Ratledge, C.; Dover, L. G., Iron metabolism in pathogenic bacteria. *Annu. Rev. Microbiol.* **2000,** *54*, 881-941.
10. Andrews, S. C.; Robinson, A. K.; Rodríguez-Quiñones, F., Bacterial iron homeostasis. *FEMS Microbiol. Rev.* **2003,** *27* (2-3), 215-237.
11. Boukhalfa, H.; Crumbliss, A. L., Chemical aspects of siderophore mediated iron transport. *Biometals* **2002,** *15*, 325-339.
12. Flo, T. H.; Smith, K. D.; Sato, S.; Rodriguez, D. J.; Holmes, M. A.; Strong, R. K.; Akira, S.; Aderem, A., Lipocalin 2 mediates an innate immune response to bacterial infection by sequestrating iron. *Nature* **2004,** *432* (7019), 917-21.
13. Holmes, M. A.; Paulsene, W.; Jide, X.; Ratledge, C.; Strong, R. K., Siderocalin (Lcn 2) also binds carboxymycobactins, potentially defending against mycobacterial infections through iron sequestration. *Structure* **2005,** *13* (1), 29-41.
14. Goetz, D. H.; Holmes, M. A.; Borregaard, N.; Bluhm, M. E.; Raymond, K. N., The Neutrophil Lipocalin NGAL Is a Bacteriostatic Agent that Interferes with Siderophore-Mediated Iron Acquisition. *Molec. Cell* **2002,** *10*, 1033-1043.
15. Harris, W. R.; Raymond, K. N.; Weitl, F. L., Ferric Ion Sequestering Agents. 6. The Spectrophotometric and Potentiometric Evaluation of Sulfonated Tricatecholate Ligands. *J. Am. Chem. Soc.* **1981,** *103*, 2667-2675.
16. Hider, R. C.; Kong, X., Chemistry and biology of siderophores. *Nat. Prod. Rep.* **2010,** *27* (5), 637-657.
17. Miethke, M.; Marahiel, M. A., Siderophore-based iron acquisition and pathogen control. *Microbiol. Mol. Biol. Rev.* **2007,** *71* (3), 413-51.
18. Raymond, K. N.; Müller, G.; Matzanke, B. F., Complexation of Iron by Siderophores. A Review of their Solution and Structural Chemistry and Biological Function. *Top. Curr. Chem.* **1984,** *123*, 49-102.
19. Crumbliss, A. L.; Harrington, J. M., Iron Sequestration by Small Molecules: Thermodynamic and Kinetic Studies of Natural Siderophores and Synthetic Model Compounds. *Adv. Inorg. Chem.* **2009,** *61*, 179-250.
20. Liu, Z. D.; Kayyali, R.; Hider, R. C.; Porter, J. B.; Theobald, A. E., Design, Synthesis, and Evaluation of Novel 2-Substituted 3-Hydroxypyridin-4-ones: Structure−Activity Investigation of Metalloenzyme Inhibition by Iron Chelators. *J. Med. Chem.* **2002,** *45* (3), 631-639.
21. Li, D. F.; Hu, P. P.; Liu, M. S.; Kong, X. L.; Zhang, J. C.; Hider, R. C.; Zhou, T., Design and synthesis of hydroxypyridinone-L-phenylalanine conjugates as potential tyrosinase inhibitors. *J. Agr. Food Chem.* **2013,** *61* (27), 6597-603.
22. Kayyali, R.; Porter, J. B.; Liu, Z. D.; Davies, N. A.; Nugent, J. H.; Cooper, C. E.; Hider, R. C., Structure-function investigation of the interaction of 1- and 2-substituted 3-hydroxypyridin-4-ones with 5-lipoxygenase and ribonucleotide reductase. *J. Biol. Chem.* **2001,** *276* (52), 48814-22.
23. Harris, W. R.; Carrano, C. J.; Cooper, S. R.; Sofen, S. R.; Avdeef, A. E.; McArdle, J. V.; Raymond, K. N., Coordination Chemistry of Microbial Iron Transport Compounds. 19. Stability Constants and Electrochemical Behavior of Ferric Enterobactin and Model Complexes. *J. Am. Chem. Soc.* **1979,** *101*, 6097-6104.
24. Gaspar, M.; Santos, M. A.; Krauter, K.; Winkelmann, G., Molecular recognition of synthetic siderophore analogues: A study with receptor-deficient and fhu(A-B) deletion mutants of Escherichia coli. *Biometals* **1999,** *12*, 209-218.

25. Meyer, J. M.; Hohnadel, D.; Hallé, F., Cepabactin from Pseudomonas cepacia, a New Type of Siderophore. *J. Gen. Microbiol.* **1989,** *135*, 1479-1487.
26. Katoh, A.; Y., H.; Harata, M.; Ohkanda, J.; Tsubomura, T.; Higuchi, A.; Saito, R.; Harada, K., 3-Hydroxy-4(1H)-pyridinone-Containing Linear and Cyclic Hexapeptides and Their Iron(III) Complexes - Synthesis, Properties and the Growth-Promotion Activity. *Heterocycles* **2001,** *55*, 2171-2187.
27. Hoette, T. M.; Abergel, R. J.; Xu, J.; Strong, R. K.; Raymond, K. N., The Role of Electrostatics in Siderophore Recognition by the Immunoprotein Siderocalin. *J. Am. Chem. Soc.* **2008,** *130*, 17584-17592.
28. Liu, Z. D.; Hider, R. C., Design of iron chelators with therapeutic application. *Coord. Chem. Rev.* **2002,** *232*, 151-171.
29. Xu, B.; Kong, X. L.; Zhou, T.; Qiu, D. H.; Chen, Y. L.; Liu, M. S.; Yang, R. H.; Hider, R. C., Synthesis, iron(III)-binding affinity and in vitro evaluation of 3-hydroxypyridin-4-one hexadentate ligands as potential antimicrobial agents. *Bioorg. Med. Chem. Lett.* **2011,** *21* (21), 6376-6380.
30. Zhang, M. X.; Zhu, C. F.; Zhou, Y. J.; Kong, X. L.; Hider, R. C.; Zhou, T., Design, synthesis, and antimicrobial evaluation of hexadentate hydroxypyridinones with high iron(III) affinity. *Chem. Biol. Drug Des.* **2014,** *84* (6), 659-68.
31. Zhou, Y. J.; Liu, M. S.; Osamah, A. R.; Kong, X. L.; Alsam, S.; Battah, S.; Xie, Y. Y.; Hider, R. C.; Zhou, T., Hexadentate 3-hydroxypyridin-4-ones with high iron(III) affinity: design, synthesis and inhibition on methicillin resistant Staphylococcus aureus and Pseudomonas strains. *Eur. J. Med. Chem.* **2015,** *94*, 8-21.
32. Qiu, D.-H.; Huang, Z.-L.; Zhou, T.; Shen, C.; Hider, R. C., In vitro inhibition of bacterial growth by iron chelators. *FEMS Microbiol. Lett.* **2011,** *314* (2), 107-111.
33. Nunes, A.; Podinovskaia, M.; Leite, A.; Gameiro, P.; Zhou, T.; Ma, Y.; Kong, X.; Schaible, U. E.; Hider, R. C.; Rangel, M., Fluorescent 3-hydroxy-4-pyridinone hexadentate iron chelators: intracellular distribution and the relevance to antimycobacterial properties. *J. Biol. Inorg. Chem.* **2010,** *15* (6), 861-77.
34. Zhou, Y.-J.; Kong, X.-L.; Li, J.-P.; Ma, Y.-M.; Hider, R. C.; Zhou, T., Novel 3-hydroxypyridin-4-one hexadentate ligand-based polymeric iron chelator: synthesis, characterization and antimicrobial evaluation. *Med. Chem. Commun.* **2015,** *6* (9), 1620-1625.
35. Xie, Y.-Y.; Liu, M.-S.; Hu, P.-P.; Kong, X.-L.; Qiu, D.-H.; Xu, J.-L.; Hider, R. C.; Zhou, T., Synthesis, physico-chemical properties, and antimicrobial evaluation of a new series of iron(III) hexadentate chelators. *Med. Chem. Res.* **2013,** *22* (5), 2351-2359.
36. Fernandes, S. S.; Nunes, A.; Gomes, A. R.; de Castro, B.; Hider, R. C.; Rangel, M.; Appelberg, R.; Gomes, M. S., Identification of a new hexadentate iron chelator capable of restricting the intramacrophagic growth of Mycobacterium avium. *Microb. Infect.* **2010,** *12* (4), 287-294.
37. Zhou, T.; Chen, K.; Kong, L. M.; Liu, M. S.; Ma, Y. M.; Xie, Y. Y.; Hider, R. C., Synthesis, iron binding and antimicrobial properties of hexadentate 3-hydroxypyridinones-terminated dendrimers. *Bioorg. Med. Chem. Lett.* **2018,** *28* (14), 2504-2512.
38. Ang, M. T. C.; Gumbau-Brisa, R.; Allan, D. S.; McDonald, R.; Ferguson, M. J.; Holbein, B. E.; Bierenstiel, M., DIBI, a 3-hydroxypyridin-4-one chelator iron-binding polymer with enhanced antimicrobial activity. *MedChemComm* **2018,** *9* (7), 1206-1212.

39. Novais, A.; Moniz, T.; Rebelo, A. R.; Silva, A. M. G.; Rangel, M.; Peixe, L., New fluorescent rosamine chelator showing promising antibacterial activity against Gram-positive bacteria. *Bioorg. Chem.* **2018,** *79*, 341-349.
40. Workman, D. G.; Hunter, M.; Dover, L. G.; Tétard, D., Synthesis of novel Iron(III) chelators based on triaza macrocycle backbone and 1-hydroxy-2(H)-pyridin-2-one coordinating groups and their evaluation as antimicrobial agents. *J. Inorg. Biochem.* **2016,** *160*, 49-58.
41. White, D. L.; Durbin, P. W.; Jeung, N.; Raymond, K. N., Specific Sequestering Agents for the Actinides. 16. Synthesis and Initial Biological Testing of Polydentate Oxohydroxypyridinecarboxylate Ligands. *J. Med. Chem.* **1988,** *31*, 11-18.
42. Seitz, M.; Moore, E. G.; Raymond, K. N., Highly Fluorescent Group 13 Metal Complexes With Cyclic, Aromatic Hydroxamic Acid Ligands. *Inorg. Chem.* **2008,** *47*, 8665-8673.
43. Jocher, C. J.; Moore, E. G.; Xu, J.; Avedano, S.; Botta, M.; Aime, S.; Raymond, K. N., 1,2-Hydroxypyridonates as Contrast Agents for Magnetic Resonance Imaging: TREN-1,2-HOPO. *Inorg. Chem.* **2007,** *46*, 9182-9191.
44. Werner, E. J.; Avedano, S.; Botta, M.; Hay, B. P.; Moore, E. G.; Aime, S.; Raymond, K. N., Highly Soluble Tris-hydroxypyridonate Gd(III) Complexes with Increased Hydration Number, Fast Water Exchange, Slow Electronic Relaxation, and High Relaxivity. *J. Am. Chem. Soc.* **2007,** *129*, 1870-1871.
45. Xu, J.; O'Sullivan, B.; Raymond, K. N., Hexadentate Hydroxypyridonate Iron Chelators Based on TREN-Me-3,2-HOPO: Variation of Cap Size. *Inorg. Chem.* **2002,** *41*, 6731-6742.
46. Streater, M.; Taylor, P. D.; Hider, R. C.; Porters, J., Novel 3-Hydroxy-2(1H)-pyridinones. Synthesis, Iron(III)-Chelating Properties, and Biological Activity. *J. Med. Chem.* **1990,** *33*, 1749-1755.
47. Piyamongkol, S.; Zhou, T.; Liu, Z. D.; Khodr, H. H.; Hider, R. C., Design and characterisation of novel hexadentate 3-hydroxypyridin-4-one ligands. *Tet. Lett.* **2005,** *46* (8), 1333-1336.
48. Workman, D. G.; Tsatsanis, A.; Lewis, F. W.; Boyle, J. P.; Mousadoust, M.; Hettiarachchi, N. T.; Hunter, M.; Peers, C.; Tétard, D.; Duce, J. A., Protection from Neurodegeneration in the 6-Hydroxydopamine (6-OHDA) Model of Parkinson's with Novel 1-Hydroxypyridin-2-one Metal Chelators. *Metallomics* **2015,** *7*, 867-876.
49. Wuts, P. G. M.; Greene, T. W., *Greene's Protective Groups in Organic Synthesis*. 4th edition ed.; John Wiley & Sons, Inc.: Hoboken, New Jersey, 2007.
50. Liu, D.; Chen, R.; Hong, L.; Sofia, M. J., Synthesis Of differentially protected phenyl d-thioglucopyranosides and 1-phenyl d-thioglucopyranosiduronic acids. *Tet. Lett.* **1998,** *39*, 4951-4954.
51. Schmidt, H.; Lensink, C.; Xi, S. K.; Verkade, J. G., New Prophosphatranes: Novel intermediates to five-coordinate phosphatranes. *Z. Anorg. Allg. Chem.* **1989,** *578*, 75-80.
52. Xu, J.; Churchill, D. G.; Botta, M.; Raymond, K. N., Gadolinium(III) 1,2-Hydroxypyridonate-Based Complexes: Toward MRI Contrast Agents of High Relaxivity. *Inorg. Chem.* **2004,** *43*, 5492-5494.
53. Formica, M.; Fusi, V.; Giorgi, L.; Guerri, A.; Lucarini, S.; Micheloni, M.; Paoli, P.; Pontellini, R.; Rossi, P.; Tarzia, G.; Zappia, G., New ligand bearing preorganized binding side-arms interacting with ammonium cations: Synthesis, conformational studies and crystal structureElectronic supplementary information (ESI) available: molecular modeling studies. *New J. Chem.* **2003,** *27* (11), 1575-1583.

54. Peuckert, F.; Ramos-Vega, A. L.; Miethke, M.; Schwörer, C. J.; Albrecht, A. G.; Oberthür, M.; Marahiel, M. A., The siderophore binding protein FeuA shows limited promiscuity toward exogenous triscatecholates. *Chem. Biol.* **2011,** *18* (7), 907-919.
55. Seitz, M.; Pluth, M. D.; Raymond, K. N., 1,2-HOIQO - a Highly Versatile 1,2-HOPO Analogue. *Inorg. Chem.* **2007,** *46*, 351-353.
56. Coutts, R. T., Catalysed Sodium Borohydride Reduction of ortho-Nitrocinnamates. *J. Chem. Soc. C* **1969**, 713-716.
57. Scarrow, R. C.; Riley, P. E.; Abu-Dari, K.; White, D. L.; Raymond, K. N., Ferric Ion Sequestering Agents. 13. Synthesis, Structures, and Thermodynamics of Complexation of Cobalt(III) and Iron(III) Tris Complexes of Several Chelating Hydroxy pyridinones. *Inorg. Chem.* **1985,** *24*, 954-967.
58. Li, Y. J.; Martell, A. E., Potentiometric and spectrophotometric determination of stabilities of the 1-hydroxy-2-pyridinone complexes of trivalent and divalent metal ions. *Inorg. Chim. Acta* **1993,** *214* (1-2), 103-111.
59. Nurchi, V. M.; Crisponi, G.; Pivetta, T.; Donatoni, M.; Remelli, M., Potentiometric, spectrophotometric and calorimetric study on iron(III) and copper(II) complexes with 1,2-dimethyl-3-hydroxy-4-pyridinone. *J. Inorg. Biochem.* **2008,** *102* (4), 684-92.
60. Andrews, J. M., Determination of minimum inhibitory concentrations. *J. Antimicrob. Chemother.* **2001,** *48* (S1), 5-16.
61. Hay, B. P.; Dixon, D. A.; Vargas, R.; Garza, J.; Raymond, K. N., Structural criteria for the rational design of selective ligands. 3. Quantitative structure-stability relationship for iron(III) complexation by tris-catecholamide siderophores. *Inorg. Chem.* **2001,** *40* (16), 3922-3935.
62. Hou, Z.; Stack, T. D. P.; Sunderland, C. J.; Raymond, K. N., Enhanced iron (III) chelation through ligand predisposition: syntheses, structures and stability of tris-catecholate enterobactin analogs. *Inorg. Chim. Acta* **1997,** *263*, 341-355.
63. Martell, A. E.; Motekaitis, R. J.; Welch, M. J., N,N',N''-Tris(3-Hydroxy-6-Methyl-2-Pyridylmethyl)-1,4,7-Triazacyclonane, a New Effective Ligand for Iron(Iii). *J. Chem. Soc., Chem. Commun.* **1990,** (24), 1748-1749.
64. Quadri, L. E.; Weinreb, P. H.; Lei, M.; Nakano, M. M.; Zuber, P.; Walsh, C. T., Characterization of Sfp, a Bacillus subtilis phosphopantetheinyl transferase for peptidyl carrier protein domains in peptide synthetases. *Biochem.* **1998,** *37* (6), 1585-95.
65. Jaya, B.; Sanjay, C., Siderophore production by clinical isolates of klebsiella pneumoniae. *Indian J. Med. Microbiol.* **1995,** *13* (1), 34-36.
66. Perry, R. D.; San Clemente, C. L., Siderophore synthesis in Klebsiella pneumoniae and Shigella sonnei during iron deficiency. *J. Bacteriol.* **1979,** *140* (3), 1129-32.
67. Gehring, A. M.; Bradley, K. A.; Walsh, C. T., Enterobactin biosynthesis in Escherichia coli: isochorismate lyase (EntB) is a bifunctional enzyme that is phosphopantetheinylated by EntD and then acylated by EntE using ATP and 2,3-dihydroxybenzoate. *Biochem.* **1997,** *36* (28), 8495-503.
68. O'Brien, I. G.; Gibson, F., The structure of enterochelin and related 2,3-dihydroxy-N-benzoyne conjugates from Eschericha Coli. *Biochim. Biophys. Acta* **1970,** *215* (2), 393-402.
69. Abergel, R. J.; Zawadzka, A. M.; Hoette, T. M.; Raymond, K. N., Enzymatic hydrolysis of trilactone siderophores: where chiral recognition occurs in enterobactin and bacillibactin iron transport. *J. Am. Chem. Soc.* **2009,** *131* (35), 12682-92.

70. Venuti, M. C.; Rastetter, W. H.; Neilands, J. B., 1,3,5-Tris(N,N',N''-2,3-dihydroxybenzoyl)aminomethylbenzene, a Synthetic Iron Chelator Related to Enterobactin. *J. Med. Chem.* **1979,** *22* (2), 123-124.
71. Pecoraro, V. L.; Wong, G. B.; Raymond, K. N., Gallium and Indium Imaging Agents. 2. Complexes of Sulfonated Catechoylamide Sequestering Agents. *Inorg. Chem.* **1982,** *21*, 2209-2215.
72. Pecoraro, V. L.; Weitl, F. L.; Raymond, K. N., Ferric Ion-Specific Sequestering Agents. 7. Synthesis, Iron-Exchange Kinetics, and Stability Constants of N-Substituted, Sulfonated Catechoylamide Analogues of Enterobactin. *J. Am. Chem. Soc.* **1981,** *103*, 5133-5140.
73. Rai, B. L.; Khodr, H.; Hider, R. C., Synthesis, Physico-chemical and lron(lll)-Chelating Properties of Novel Hexadentate 3-Hydroxy-2(1H)pyridinone Ligands. *Tetrahedron* **1999,** *55*, 1129-1142.
74. Fish, W. W., Rapid colorimetric micromethod for the quantitation of complexed iron in biological samples. . *Methods Enzymol.* **1988,** *158*, 357-364.
75. Skoog, D. A.; West, D. M.; Holler, F. J.; Crouch, S. R., In *Analytical Chemistry: an Introduction*, 7th ed.; Saunders College Division: 2000.
76. Gans, P.; O'Sullivan, B., GLEE, a new computer program for glass electrode calibration. *Talanta* **2000,** *51* (1), 33-37.
77. Gans, P.; O'Sullivan, B. *GLEE*, 3.0.15; Protonic Softwares: Leeds, UK; Berkeley, CA, 2005.
78. Gans, P.; Sabatini, A.; Vacca, A., Investigation of equilibria in solution. Determination of equilibrium constants with the HYPERQUAD suite of programs. . *Talanta* **1996,** *43*, 1739-1753.
79. Alderighi, L.; Gans, P.; Ienco, A.; Peters, D.; Sabatini, A.; Vacca, A., Hyperquad simulation and speciation (HySS): a utility program for the investigation of equilibria involving soluble and partially soluble species. . *Coord. Chem. Rev.* **1999,** *184*, 311-318.
80. Baes, C. F.; Mesmer, R. E., *The Hydrolysis of Cations*. John Wiley & Sons: New-York, 1976.
81. Gillet, R.; Roux, A.; Brandel, J.; Huclier-Markai, S.; Camerel, F.; Jeannin, O.; Nonat, A. M.; Charbonniere, L. J., A bispidol chelator with a phosphonate pendant arm: synthesis, Cu(II) complexation, and 64Cu labeling. *Inorg. Chem.* **2017,** *56*, 11738-11752.
82. Wang, J.; Chen, X.; Su, L.; Li, P.; Cai, Q.; Liu, B.; Wu, W.; Zhu, Z., MicroRNA-126 inhibits cell proliferation in gastric cancer by targeting LAT-1. *Biomed. Pharmacother.* **2015,** *72*, 66-73.